Comal Springs Riffle Beetle Population Assessment

Final Report

February 2025

Prepared By:

Matthew R. Pintar
Kyle T. Sullivan
BIO-WEST, Inc.
1405 United Drive, Suite 111
San Marcos, Texas 78666

Prepared For:

Edwards Aquifer Authority
900 East Quincy Street
San Antonio, Texas 78215

Contents

1. Executive summary

Over the past decade, much progress has been made in understanding the biology of the endangered Comal Springs Riffle Beetle (*Heterelmis comalensis*; CSRB). Despite the advances provided by studies of the species in captivity and the wild, there has been little clear evidence of what environmental habitat characteristics affect CSRB abundance and occupancy in natural spring sites. This in turn has limited the ability to use data collected during semiannual biomonitoring to inform on the status of the species. The goal of this project was to conduct a study of the CSRB population across the Comal Springs system to 1) generate an understanding of the environmental habitat variables that relate to CSRB relative abundance and apparent occupancy and 2) develop model-based relative abundance estimates that can be used to inform biological monitoring.

Over a 13-month period from April 2023 to May 2024, five sampling events were conducted at 83 sites across the Comal Springs system. Various measures of site-specific habitat quality, such as water quality, organic material presence, and springflow were directly quantified. Additional local measures of springflow were generated using local discharge measurements from long-term monitoring data and total system springflow from USGS data. Generalized linear mixed effects models were developed for adult and larval CSRB, along with a similar co-occurring but non-spring-endemic species, *Microcylloepus pusillus*, for comparison. The Spring Island area supported the highest relative abundances of CSRB and was also the locality with the overall most stable habitat (consistent springflow), while Spring Run 3 and the Western Shoreline supported lower relative abundances of CSRB. Relative abundances were near-zero in Spring Run 1, where all sampled sites dried during summer 2023, and no CSRB were found in the Upper Spring Run.

Model results indicated that of the examined covariates, local springflow, or springflow attributed to each locality within the system (e.g., Spring Run 1, Spring Run 3, subsections of Spring Island), had the largest positive effect on relative abundance and apparent occupancy of CSRB. The only other covariate with an effect included in the final model was total biofilm coverage of cotton lures, which also had a positive effect for both life stages. These CSRB model results contrast with those of *M. pusillus*, for which there was no response to springflow or biofilm. Although this project included one of the periods of lowest total system springflow during the preceding 30 years, the range of conditions experienced over the course of the project provided environmental variation that informed the model of the effects of springflow on CSRB populations. The model results are perhaps more critical to the understanding of how CSRB are affected by environmental conditions given the potential for future long-term shifts towards lower system-wide flows as anthropogenic effects on the ecosystem grow.

The results of this study and its models have been adapted into a framework that can be used to assess the status of CSRB populations through the biological monitoring program. This framework can determine whether CSRB relative abundances are within historic norms and if observed relative abundances meet expectations based on observed values for environmental covariates. This study emphasizes the need for maintaining adequate springflow across localities to support each CSRB subpopulation. Additional study is needed to measure CSRB responses to higher springflows, assess if there is any true subsurface habitat use, and determine any drivers of lure biofilm.

2. Introduction

The Comal Springs Riffle Beetle, *Heterelmis comalensis* (CSRB; Coleoptera: Elmidae), was initially described as a species endemic to Comal Springs in Comal County, Texas (Bosse et al. 1988). It was later found 28 km away in San Marcos Springs, Hays County (Gibson et al. 2008), but it has not been found in smaller springs throughout the region. Much less is known regarding the smaller, isolated CSRB population in San Marcos Springs and its relationship to the Comal Springs population; only the Comal Springs population is considered here.

CSRB are brachypterous, meaning they have incompletely developed, non-functional wings (Bosse et al. 1988). The loss of wings is likely an adaptation to conserve resources (Zera and Denno 1997) in the stable environmental conditions provided by what historically has been the largest spring complex by discharge in Texas (Brune 2002), and in turn CSRB, as a species, are reliant on this spring system. In 1997, this led to listing CSRB as federally endangered, as the species is threatened by the combination of their limited distribution and increasing human development above the Edwards Aquifer (USFWS 1997). In particular, the species is threatened by excessive human withdrawal of water from the aquifer (USFWS 1997). There is also a recognized risk to the species if groundwater contamination were to occur (Bowles and Arsuffi 1993; USFWS 1997), although evidence for contamination of the aquifer has been minimal (Hutchins 2018). During the drought of record in the 1950s, CSRB presumably survived in hyporheic habitats, but it is unknown how adversely the species was affected or how long it took to recover. A total of 22 ha of surface habitat have been designated as critical habitat – habitat that is essential for a species' conservation – for CSRB in the Comal Springs system (USFWS 2013). A recent review of the species found no need for status change, stating that it remains at risk due to water withdrawals and land use change (USFWS 2024).

Following the listing of CSRB, a biological monitoring program with standardized semiannual sampling was initiated in 2004, and further conservation actions have been taken as part of the Edwards Aquifer Habitat Conservation Plan (EAHCP). An initial field survey (Bowles et al. 2003) did not find clear microhabitat associations of the species, but further work confirmed a spring association of CSRB across small distances (Cooke et al. 2015). A wide range of other studies have been undertaken to understand the species, which along with several unpublished reports and theses (full extent of work summarized in USFWS 2024), include publications on its diet (Nair et al. 2021), microbiome (Mays et al. 2021), response to environmental conditions (Nair et al. 2023), and its life history (Fries 2003, Huston and Gibson 2015, Kosnicki 2022). Life history research has led to the establishment of reproducing captive populations that could be used for reintroduction if a catastrophic event were to occur in the wild (USFWS 2022).

Despite 20 years of CSRB biomonitoring and extensive study of other aspects of its biology, little remains known about environmental factors that affect CSRB habitat occupancy and abundance in the wild. Mark-recapture has proven ineffective (Huston et al. 2015), females are seemingly continuously iteroparous (Kosnicki 2022), and there is a lack of seasonal phenological differences in the presence and abundance of each life stage (Bowles et al. 2003). These factors, along with the potential effects of springflow (drying sites) on CSRB, have made it difficult to study this species using many of the traditional methods used for assessing species occupancy and population size.

Given the challenges of studying wild CSRB populations, planning for a population study was initiated in 2021 under the guidance of the EAHCP Science Committee CSRB working group. The study was designed to assess CSRB across the Comal Springs system using more rigorous and spatially expansive surveys than were used in previous studies and in semiannual biomonitoring, while repeating surveys at the same sites multiple times over the course of one year and quantifying potential environmental covariates. The primary objectives of this study were to 1) generate an understanding of what environmental covariates relate to CSRB abundance and 2) develop model-based relative abundance estimates that can be used to inform biological monitoring.

3. Methods

3.1 Field methods

3.1a Sample sites and schedule

Sampling for CSRB was conducted using cotton lures at 83 sites across the Comal Springs system during a 13-month period beginning in April 2023 and ending in May 2024. We used the cotton lure methodology that was standardized following EAHCP implementation and is a modification of a previous method that utilized a similar-sized piece of cloth but was not folded into a cage. The cotton lure consists of a 15 cm × 15 cm square piece of 200 thread count cloth (60% cotton and 40% polyester) folded by thirds and placed into a 4 cm × 4 cm wire cage made from galvanized wire (Edwards Aquifer Authority 2016). At spring openings that had noticeable springflow, lures were placed just below the substrate—water interface and covered rocks to hold in place and block light from the lure (CSRB avoid light; Cooke et al. 2015).

Lures were left in situ for approximately 30 days (standard since 2004), allowing for colonization and growth of biofilm on each lure, which serves as a food source and potential attractant that encourages colonization of the lures by CSRB. Longer deployment of lures often leads to degraded lures that experience greater/earlier biofilm colonization and in turn fewer CSRB since the lure no longer retains its structure (Huston et al. 2015). Upon retrieval, any lures that were disturbed (e.g., dug up by raccoons or humans, or cloth pulled from the cage by crayfish), exposed to light, experienced heavy sedimentation (historically from heavy precipitation), dried out due to declining water levels, or were otherwise lost, were excluded from analyses.

The sampling schedule was planned so that three of the five sampling periods coincided with spring and fall CSRB biomonitoring (sampling periods 1, 3, and 5; Table 1). The first sampling period occurred when lures were set in April 2023 and retrieved in May 2023. Subsequent sampling periods began approximately two months after the preceding sampling period (Table 1). Lures were set and retrieved over a 2–4-day period.

This study coincided with one of the periods lowest total system springflow in 30 years. Although total system springflow during this study was generally low, it exhibited considerable variation across all of the study periods, with a maximum of 205 cubic feet per second (cfs) in January 2024 and a minimum of 66 cfs in July 2023 (Fig. 1). This variation in flow is important for the interpretation and applicability of results, as the range of conditions experienced during the study inform the models, and the conditions experienced outside of this range necessitate extrapolation of the model, which may not necessarily produce accurate results.

During spring 2023, the decision was made to proceed with this study over concerns about prolonged low-flow conditions because 1) effects of flow on CSRB during low-flow periods are probably more important to understanding CSRB populations than are only conditions within typical historic ranges, especially in the context of climate change, continued land use change, and potential long-term declines in springflow, and 2) there was no way to confidently predict future flows and plan to conduct the study under historically normal conditions. This is further emphasized by the conditions that occurred after the study end, during the nine months from May 2024 through February 2024, which exhibited both lower average springflow than during the study, and perhaps more critically, these months had less variation in springflow than observed during the study period.

Table 1. List of sampling periods with the start and end dates (earliest date lures were set, latest dates lures were retrieved) and the mean 30-day total system springflow over each sampling period.

Sample period	Start date	End Date	Mean 30-day springflow (cfs)
1	10 April 2023	10 May 2023	140
2	5 July 2023	9 August 2023	83
3	23 October 2023	21 November 2023	110
4	29 January 2024	1 March 2024	183
5	15 April 2024	17 May 2024	147

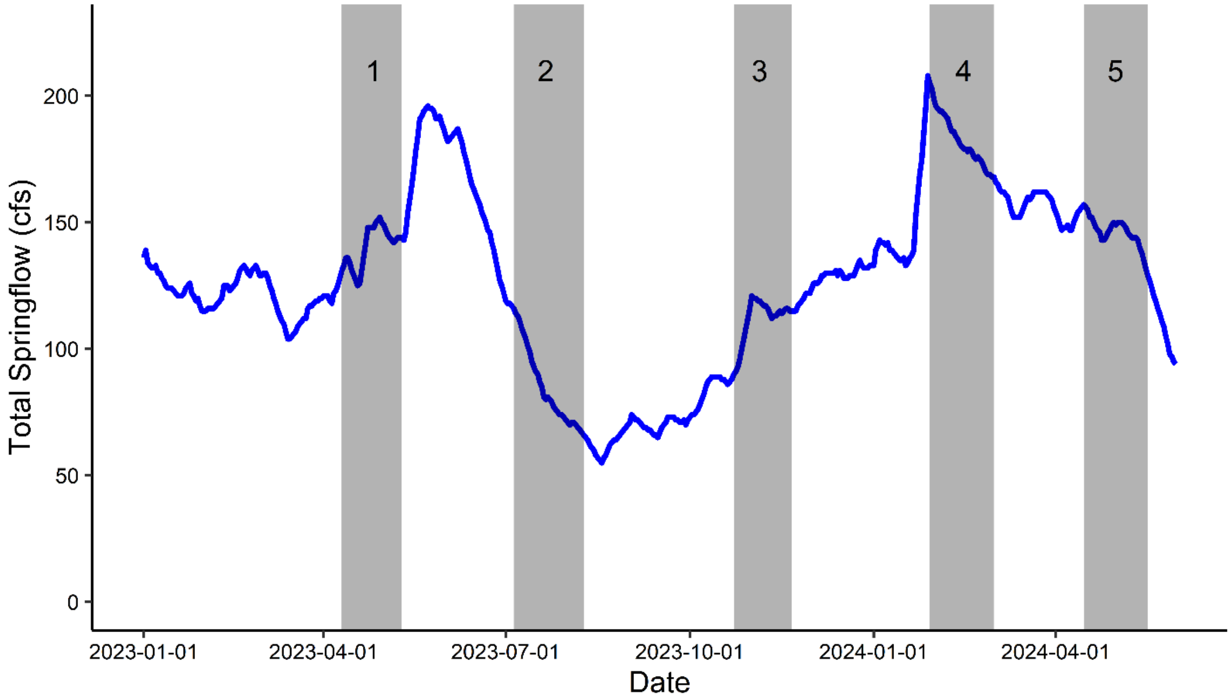

Figure 1. Daily total system springflow from Comal Springs from the start of 2023 through spring 2024 with gray shaded areas representing the five sampling periods (sampling periods 1–5; Table 1).

Initially, 80 sites were selected across five localities in the Comal Springs system. This included the 30 sites used for semiannual biomonitoring, which encompassed ten sites each in these localities: Spring Island, Spring Run 3, and the Western Shoreline. Fifty additional sites were added with ten sites each in these five localities: Spring Island, Spring Run 1, Spring Run 3, Western Shoreline, and the Upper Spring Run area (Fig. 2). Lucas et al. (2016) proposed three CSRB subpopulations based on molecular data: Spring Run 1, Spring Run 3, and Western Shoreline + Spring Island. We planned the sampling design around these subpopulations by balancing availability of active springs and spatial coverage of sites at each locality. Spring Run 2 was excluded because it was expected to have fewer active springs and was considered under recovery from restoration activities. The Upper Spring Run (headwaters) area was added to the study to determine the status of CSRB in that locality since it has not been as extensively studied as the rest of the system.

The additional 50 sites were initially randomly selected from known spring sites mapped by the Texas Parks and Wildlife Department (unpublished data), although their mapped sites were not representative of all active springs. Selected sites were modified when setting the initial group of lures in April 2023 to ensure that lures were set in active spring sites while balancing adequate spatial coverage across each locality and attempting to set lures within close proximity to randomly selected sites. Two additional sites were added in the Upper Spring Run for the final two sampling periods because more sites had active springflow during those sampling periods and we wanted expand the sampling effort to potentially detect CSRB in that locality. Lastly, one of the initial sites at the Western Shoreline was lost due to heavy sedimentation from construction by landowners on the hill above the site; sampling for the remaining two periods was moved to a nearby site (~10 m) that was unaffected by sedimentation.

Upon lure retrieval, lures were inspected and all macroinvertebrates were removed and examined using a microscope. Adult and larval CSRB and *Microcylloepus pusillus* (MIPU) were identified and counted; other spring-associated invertebrates (*Stygoparnus comalensis*, *Stenelmis sexlineata*, *Stygobromus* spp., *Lirceolus* spp.) were counted but are not otherwise considered here because the cotton lure sampling method is not specifically targeted towards these species and their abundances were too low for meaningful analysis. Most of the invertebrates were returned to their spring of origin after enumeration. Some CSRB larvae and less than 50% of adults were preserved in ethanol and transferred to USFWS San Marcos Aquatic Resources Center for genetic analysis; collection restrictions were placed by EAA to limit potential effects on the population study. Given high rates of overdispersion and low rates of recapture (<1%; Huston et al. 2015), it is not expected that this limited removal of CSRB from the system had any impact on subsequent counts.

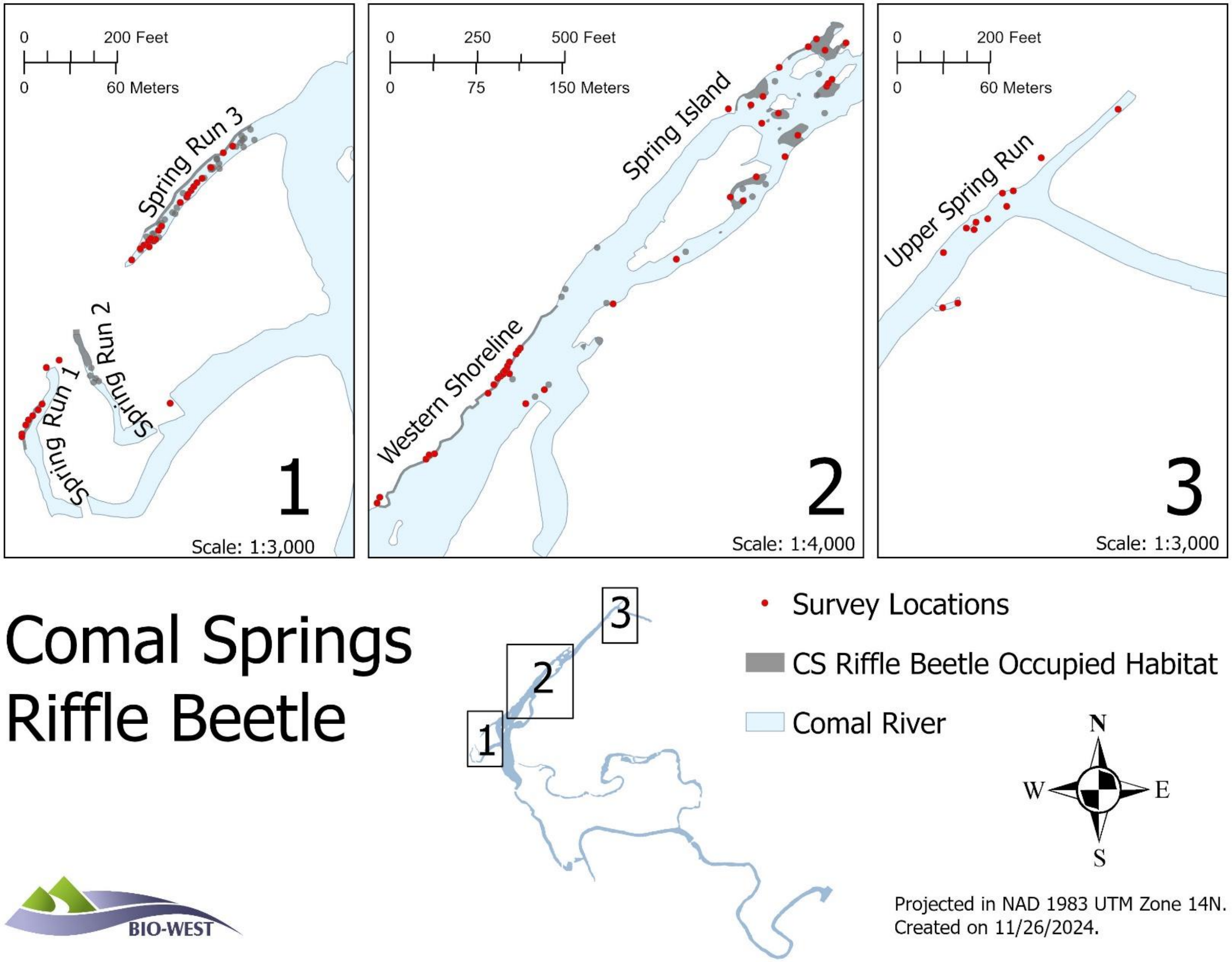

Figure 2. Map of the 83 sample locations (red dots) throughout the Comal Springs with CSRB occupied habitat (gray area; areas where CSRB have been recorded in the past ten years).

3.1b Covariates

At the time of lure set and/or lure retrieval we collected or calculated several spring-level, lure-level, and higher-level (locality or total-system) covariates. Water temperature, dissolved oxygen, conductivity, and pH were measured at lure set and retrieval with a YSI Professional Plus meter. Two measures of depth were collected at both lure set and lure retrieval: water depth was the distance from the water surface to the substrate surface (sometimes negative = substrate above water surface) and lure depth was the distance from the water surface to the lure. Lure depth was always positive when set (underwater), but sometimes negative (above water) when retrieved; any lures above the water when retrieved were excluded. The average substrate size was calculated when lures were set: the percent silt, sand, and boulder/bedrock (anything >256 mm) were estimated and a subsample of all other intermediate size substrate particles were individually measured. We also recorded at both lure set and retrieval whether four categories of organic material were present within the spring area: dead tree wood, dead tree leaves, tree roots, and live macrophytes or bryophytes. Wood, leaves, and roots were combined into an aggregate organic material presence/absence variable.

Site-level springflow (at each lure location) was measured via two methods at both lure set and lure retrieval. A Hach portable velocity meter was used to measure the water velocity (flow) at each terrestrial margin and orifice site, as well as at rocky upwelling sites. Initial (pre-study) investigation into more complex measurements of springflow using multiple recordings over a measured area at terrestrial margin sites using the Hach flow meter did not produce meaningfully different results than a single point measurement. This was likely due to the small area over which there is springflow at each site, the proportionally large area of the Hach probe relative to the lure and most spring openings, and the sensitivity of the probe to slight change in angles in these low-velocity springs. Similarly, during pre-study preparation and examination of sites, it was clear that measurements obtained from the Hach flow meter in upwelling sites were not consistent or reliable due to the influence of both lateral movement of water, proximity of the probe to the spring opening, and force of larger amounts of water impeding our ability to obtain flow measurements at deeper sites that were obviously flowing based on visual observations. Over 90% of flow meter measurements in upwelling sites were, as recorded by the Hach velocity meter, between 0 and 0.09 ft/s (the Hach meter has an accuracy of 0.01 ft/s).

To measure water flux from upwelling sites, a seepage meter was constructed from a circular bucket (diameter = 15 cm, area = 176.7 cm^2) attached to a garden hose with a valve and plastic bag for water collection (Appendix Fig. S1). Water was drained from the bag and air was purged from the system prior to each measurement. The seepage meter bucket was inserted into the substrate to isolate the spring opening, the valve opened, and the bag allowed to fill for 30–60 s. This process was repeated at each site three times within a ten-minute period, and the three measurements ($mL/cm^2/s$) were averaged. To make measurements comparable between the two methods, for 51 of the seepage meter measurements, we also measured the flow of water from each upwelling with the Hach flow meter. Of the 51 measurements, one standard deviation nearly overlapped with 0 (1.64 ± 1.32 cm/s) for the Hach flow meter measurements but was more than two standard deviations from zero when using the seepage meter (0.15 ± 0.06 $mL/cm^2/s$), suggesting the seepage meter effectively isolated water flowing from each spring site and produced a more meaningful number than the flow meter. We then compared the seepage meter flux to the flow meter reading and then converted the flux at each site to a flow measurement based on the linear relationship between these two variables (Appendix Fig. S2; flow = 12.909 × flux – 0.2902).

After each lure was retrieved and invertebrates removed, the lure was spread out on a white background and photographed (Fig. 3). The percent coverage of biofilm on the lures was then visually estimated for each of these colors: black, orange, yellow, purple, and green. Green, which may have been suggestive of light exposure and photosynthesis, only accounted for 5% coverage on a single lure. Total biofilm coverage (all colors summed) was used a final covariate in analyses. A total of 15 lures had their biofilm manually calculated by outlining each color patch and calculating the percentage coverage of each lure, however this procedure was not perfect due to overlap and intergrowth of different biofilm colors. It also took considerably more time and did not meaningfully differ from visual estimation. Lastly, we tried using automated color counting programs, but these tools could not distinguish discoloration from sediment from biofilm. It is also likely that non-visible biofilms cover parts of each lure, but we consider visual discoloration by biofilms to be representative of overall biofilm abundance.

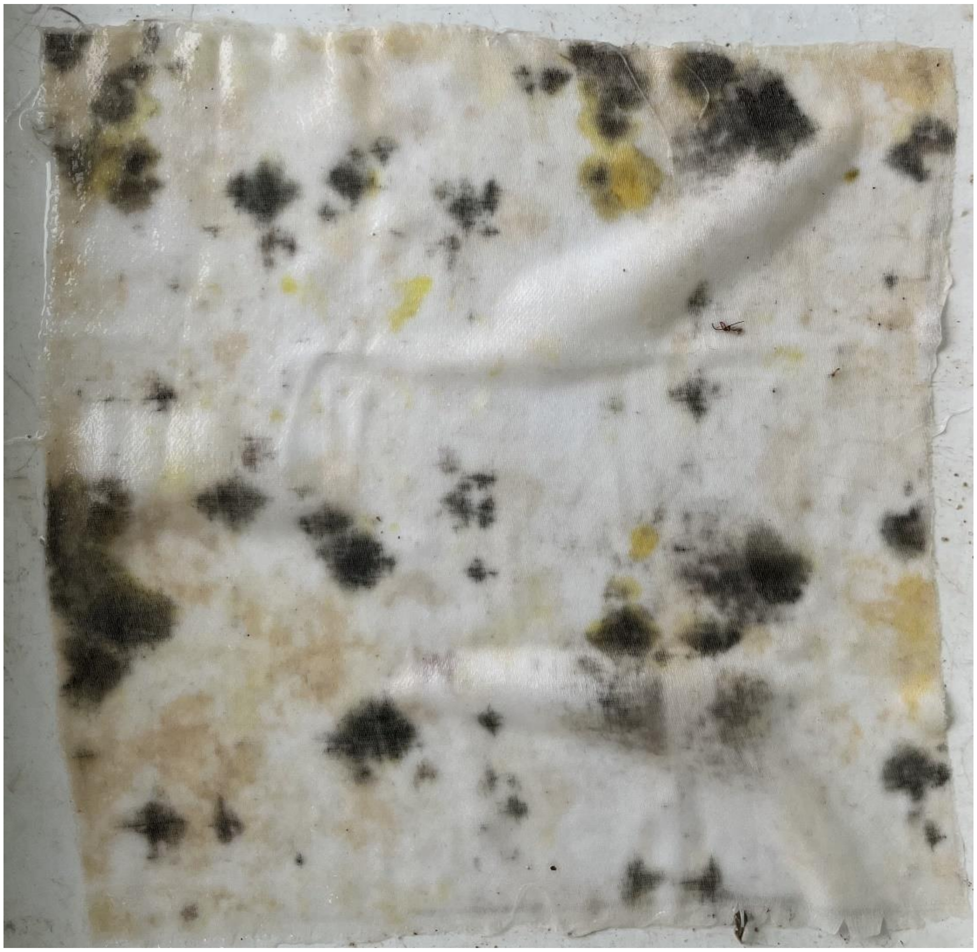

Figure 3. Photograph of one lure after retrieval exhibiting black, yellow, orange, and a small patch of purple biofilm (often blends in with black).

Because biofilm accumulates on lures and then degrades the lures as they remain in the system for longer periods of time, we initially explored using the number of days each lure was set in the system as a covariate. However, such temporal variation is usually observed with data from over longer time spans (10–60 days), and the number of days our lures were set had a much smaller range (26–35 days) with a mean of 30 days and standard deviation of 2.2 days.

We also explored the use of total system covariates such as total system springflow and precipitation, but these were ultimately dropped in favor of localized springflow (see section 3.2b below). Within each locality (Spring Island, Spring Run 1, Spring Run 3, and Western Shoreline), we created spatial groupings (sectors) of sites based on spatial proximity and similarity of sites (Appendix Figs. S3–S5). This was initially done to account for potential spatial autocorrelation in CSRB populations or environmental conditions, but ultimately it was only used to generate measures of local springflow.

For all of the covariates measured or calculated, we visually explored and interpreted the data, incorporated knowledge of the ecology of the Comal Springs system, and used automated model selection on initial generalized linear mixed effects models with the *dredge* function in the 'MuMIn' (Bartoń 2020) package in R (R Core Team 2024) to generate an initial set of final covariates. These final covariates were then included in the final model formulation and refined to achieve final models.

3.2 Statistical methods

The overall goal of this study component was to develop generalized linear mixed effects models (GLMMs) under a Bayesian framework to better understand what environmental factors influence patterns CSRB adult relative abundance and apparent occupancy. Specific objectives included: 1) assess variation of CSRB relative abundance between study sites; 2) quantify the effects of local springflow and biofilm on CSRB relative abundance; 3) derive apparent occupancy probability estimates for objectives 1–2; 4) fit GLMMs for CSRB larvae, and MIPU adults and larvae for comparison; and 5) develop a framework to demonstrate how GLMMs can be used as a tool for the EAHCP Biological Monitoring Program.

Other methods for assessing population sizes were considered during study design and explored in preliminary analyses, but ultimately were excluded because they produced either highly variable population estimates and/or violated statistical assumptions needed to obtain valid results. In particular, *N*-mixture models (Royle 2004) are commonly used in vertebrate surveys to estimate population sizes based on spatially replicated count surveys. However, this study of CSRB populations violated *N*-mixture models in two ways. The CSRB populations within each site were not closed, with the potential for movement to/from sites as well as births and deaths due to the short lifecycle (egg to adult in 6–12 months; USFWS 2024). Additionally, our data, and insect populations in general, tend to be over-dispersed and do not conform to the requirements of *N*-mixture models. Both of these assumptions that are necessary for *N*-mixture models can be relaxed in GLMMs to effectively model CSRB relative abundance.

3.2a Relative abundance model formulation

Patterns in CSRB and MIPU relative abundance were investigated by fitting overdispersed Poisson GLMMs (Breslow 1984). The same model structure was used of each species and life stage and formulated as follows:

$$y_{i,t,j} \sim Poisson(\lambda_{i,t,j}),$$

where $y_{i,t,j}$ is the observed relative abundance (counts/lure) for lure sample *j* during sampling event *t* at site *i*, and was assumed to be the outcome of a Poisson distribution with an expected value of $\lambda_{i,t,j}$. For each GLMM, a log link was used to regress expected values with a linear equation:

$$log(\lambda_{i,t,j}) = \alpha_i + \beta_1 local.springflow_{i,t,j} + \beta_2 total.biofilm_{i,t,j} + \varepsilon_{i,t,j},$$

where α_i is the intercept for site *i*, β_1 is the slope for the effect of 30-day local springflow average (cfs), β_2 is the slope for the effect of total biofilm (%), and $\varepsilon_{i,t,j}$ is an extra-residual term to accommodate additional site-event-sample dispersion. Methods for deriving 30-day local springflow average are described in Section 3.2b.

Site-level intercepts were assumed to be drawn from a Normal distribution with a population-level mean (μ_α) and variance (σ_α^2):

$$\alpha_i \sim Normal(\mu_\alpha, \sigma_\alpha^2)$$

Extra-residual random effects were assumed to be drawn from a Normal distribution with a mean of zero and site-event-sample variance (σ_ε^2):

$$\varepsilon_{i,t,j} \sim Normal(0, \sigma_\varepsilon^2)$$

Since occurrence is also a state variable of interest, apparent occupancy probability was estimated as a derived quantity to assess how it varies between sites and visualize its relationship with environmental covariates. Occupancy was considered apparent because true occupancy is confounded with detection (Kéry et al. 2010). So, like relative abundance, apparent occupancy is an index. Where applicable, estimates of apparent occupancy probability (ψ) were derived directly from relative abundance (λ) estimates using the following 1:1 function:

$$\psi = \Pr(y > 0 \mid \lambda) = 1 - e^{-\lambda},$$

where $e^{-\lambda}$ is the expected probability that relative abundance is equal to zero (Royle and Dorazio 2008).

3.2b Local springflow covariate derivation

Local springflow was derived using spring discharge data from two sources. First, discharge (cfs) data measured from eight stations in Comal Springs were obtained from the EAHCP biological monitoring program (Fig. 4). These data were collected from 2003–2024 in spring and fall of each year. Measurements were also conducted in summer when system-level river discharge decreased to specific low-flow thresholds outlined in the EAHCP (2012). Second, mean daily discharge (cfs) data from the Comal Springs USGS stream gage (#08168710; 1938–2024) were gathered using the R package 'dataRetrieval' (De Cicco et al. 2024).

A linear mixed effects model (LMM) was fit to predict local springflow using the R package 'glmmTMB' (Brooks et al. 2017). Discharge measurements at the eight monitoring stations described above was the response variable and Comal Springs mean daily discharge (hereafter 'total system springflow') on the date of station measurements was the predictor variable. Regression coefficients were estimated for each station by including station as a group-level predictor (i.e., random effects) that allowed their intercepts and slopes to vary randomly. For analysis, total system springflow was centered using the long-term average (1938–2024). Model performance was assessed based on conditional variance explained (R^2) and root mean squared error (RMSE). In addition, 10-fold cross-validation was conducted to evaluate how well the LMM generalizes to out-sample-data ($RMSE_{cv}$) and was estimated by calculating mean (± standard error) predictive accuracy across test folds. All LMM performance statistics and parameter estimates (± standard error) were summarized in a table. Relationships between station discharge and total system springflow were predicted using the R package 'ggeffects' (Lüdecke 2018) and visualized using the R package 'ggplot' (Wickham et al. 2024).

To link local springflow to CSRB lure sample data, a discharge time-series was predicted for stations closest to each site over the study period and 30-day local springflow average was calculated on the date of lure retrieval to approximate springflow conditions for the duration each lure was set. Local springflow at Spring Island was based on stations in closest proximity to each of its four sectors. Lastly, local springflow at Western Shoreline was approximated by subtracting Landa Lake Cable discharge from total springflow (Table 2). While this calculation also includes flow contributions from spring upwellings throughout the lake, it provides a more realistic approximation of springflow conditions at Western Shoreline compared to discharge at Landa Lake Cable exclusively.

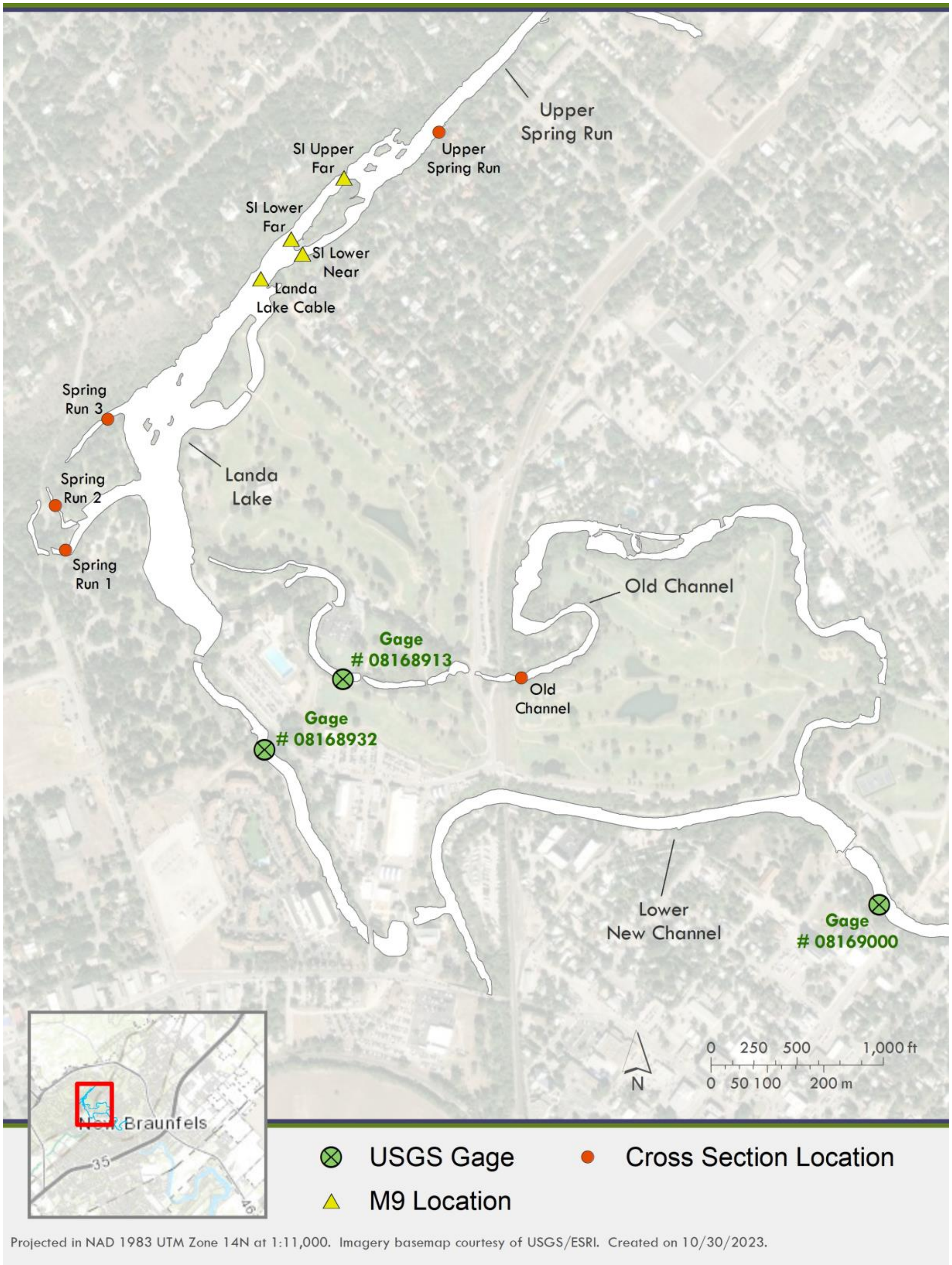

Projected in NAD 1983 UTM Zone 14N at 1:11,000. Imagery basemap courtesy of USGS/ESRI. Created on 10/30/2023.

Figure 4. Locations of stations used to local springflow discharge Comal Springs. Cross section springflow measurements were conducted using a HACH FH90 flowmeter and adjustable wading rod. Spring at M9 locations were measured with an acoustic doppler device used by the Edwards Aquifer Authority.

Table 2. Springflow discharge stations used to assess local springflow effects on CSRB relative abundance at each sector per site (see Appendix Figs. S3–S5 for sectors).

Site (sector)	Station
Spring Island (A, D)	Spring Island Lower Near
Spring Island (B, C)	Spring Island Upper Far
Western Shoreline (A–D)	Total Springflow - Landa Lake Cable
Spring Run 3 (A–C)	Spring Run 3
Spring Run 1 (A–C)	Spring Run 1

3.2c Relative abundance model analysis and inference

All GLMMs were analyzed by means of a Bayesian framework with Markov Chain Monte Carlo (MCMC) methods using JAGS called from the R package 'jagsUI' (Kellner 2024). All priors were parameterized to express our current lack of knowledge about each parameter (Hobbs and Hooten 2015). Weakly informative normal prior distributions were used for the population-level mean and slopes for each covariate. Vague uniform prior distributions were used for all variance parameters. Before analysis, total biofilm was centered by its overall mean and 30-day local springflow discharge was centered using site-specific means. Posterior distributions for each parameter were estimated based on the 3rd sample from 80,000 iterations of three chains with a burn-in period of 20,000 iterations per chain. Model convergence was assess based on visual inspection of trace plots, the Gelman-Rubin statistic ($\check{R}$), and density plots for each parameter. Convergence was considered successful if trace plots showed good mixtures of MCMC chains, if $\check{R}$ was less than 1.1 (Gelman and Rubin 1992), and density plots showed similar shapes for each chain.

Multiple methods were used to evaluate model performance. Posterior predictive checks were used to assess consistencies in goodness-of-fit between observed and simulated data. Bayesian *p*-values (B_p) were calculated using the chi-squared discrepancy statistic to estimate the probability that fit of simulated data (χ^2_{sim}) was more extreme than observed data (χ^2_{obs}). Bayesian *p*-values close to zero or one indicated a lack of model fit (Gelman et al. 2013, Hobbs and Hooten 2015). Root mean squared error was also calculated for observed ($\mathrm{RMSE}_{\mathrm{obs}}$) and simulated ($\mathrm{RMSE}_{\mathrm{sim}}$) data as an additional measure of posterior predictive accuracy. Further, marginal and conditional R^2 were calculated to quantify variation explained by each model based on methods for GLMMs described by Nakagawa and Schielzeth (2013). Lastly, 10-fold cross validation was conducted to evaluate how the models generalize to out-sample-data. Predictive accuracy across test folds ($\mathrm{RMSE}_{\mathrm{cv}}$) was estimated using the R package 'jagshelper' (Tyers 2024).

Parameter estimates were based on the median of their posterior distributions and were qualified by uncertainty using 90% Bayesian credible intervals (BCIs). Summaries of all parameter estimates for each model are presented in a table. Site-level intercepts were visualized to assess spatial variation in mean relative abundance on its original scale (counts/lure) and apparent occupancy probability. Lastly, covariate relationships with relative abundance and apparent occupancy were visualized for slopes with

BCIs that did not overlap with zero. All graphical results were built using the R package ‘ggplot2’ (Wickham et al. 2024).

3.3d Framework for biological monitoring applications

The proposed framework aims to demonstrate how the GLMM formulated for this study can be used as a tool for the EAHCP Biological Monitoring Program to assess whether observed relative abundances of CSRB at a given time period met expectations. For CSRB, relative abundance can be used to assess population trends under the following assumptions: 1) relative abundance is a reasonably accurate representation of the population at each site; 2) sampling data are representative of the population – location of samples per monitoring event are selected in a manner that grants inference about each site (including locations not sampled); and 3) the GLMM is a reasonable description of the data, is able to mimic the data with acceptable accuracy, and can adequately generalize to new data.

To exemplify this approach, data collected during the fall 2024 EAHCP monitoring event were used to forecast relative abundance of CSRB adults. Lures were set for 27 days (8 October – 4 November) at Spring Island and 30 days (7 October – 6 November) at Western Shoreline and Spring Run 3 (10 lures in each locality; n = 30 lures total). Mean daily total system springflow during the duration lures were set ranged from 55–74 cfs and total biofilm on the day of lure retrieval ranged from 10–85%. A schematic of the proposed framework is illustrated in Fig. 5 and involves three general steps. For step one, 30-day local springflow average was first derived for each lure sample using the methods described in Section 3.2b. Expected values of each lure sample were then forecasted given their covariate values and the GLMM parameter estimates. Specifically, a posterior forecast distribution was generated by predicting relative abundance from each MCMC posterior sample for site-level intercept and covariate effect sizes (Hobbs and Hooten 2015).

For step two, model fit was first assessed by estimating RMSE (90% BCI) and visually inspecting residuals for fall 2024 predictions. Residual inspections included plotting a histogram and scatterplots for residuals versus predictions and each covariate fit using quantile regression (quantile = 0.5). Observed and expected CSRB adult relative abundance were then summarized at each site for comparison. First, median observed relative abundance was calculated for each site as a measure of population state and was compared to each sites median forecast estimate and its associated 90% BCI. Boxplots were also used to provide visual comparisons between observed relative abundance and posterior forecast distributions for each site. Outliers were omitted from each boxplot to help with interpretability. All residual diagnostic graphs and boxplots were built using the R package ‘ggplot2’ (Wickham et al. 2024).

Lastly, step three uses results from step two to answer the following question: does the observed data agree with expectations? If the answer was yes, it would be concluded that observations were most likely attributed to covariate effects. If expectations were not met, this would suggest residual relative abundance was potentially a response to other deterministic or stochastic processes not accounted for in the GLMM.

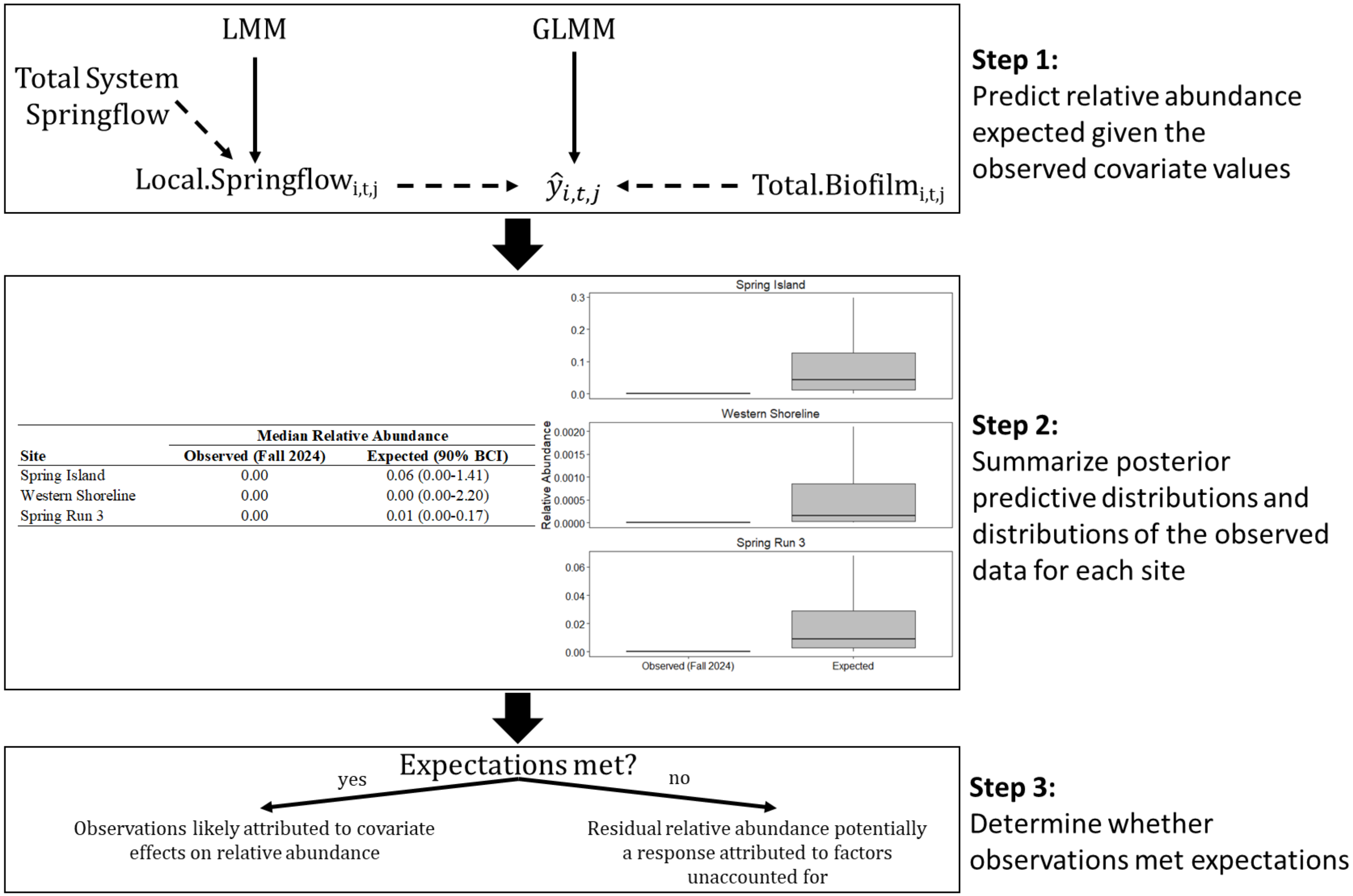

	Median Relative Abundance	
Site	**Observed (Fall 2024)**	**Expected (90% BCI)**
Spring Island	0.00	0.06 (0.00-1.41)
Western Shoreline	0.00	0.00 (0.00-2.20)
Spring Run 3	0.00	0.01 (0.00-0.17)

Figure 5. A schematic of the proposed conceptual framework illustrating how generalized linear mixed effects models can be used as a tool for assessing Comal Springs Riffle Beetle populations under the EAHCP Biological Monitoring program.

4. Results

4.1 Field measurements

4.1a Beetles recorded

Out of a total of 404 lures set during the study, 13 were lost due to disturbance and 38 were dry at the time of retrieval, resulting in 353 lures (samples) with complete data. All dry lures were found during the sampling period 2 (summer 2023) when total system springflow dropped dramatically from the start of the sampling period to the end (Fig. 1). In total, over 600 adults of both CSRB and MIPU were found, with the highest numbers around Spring Island, fewer at Spring Run 3 and the Western Shoreline, and only a single CSRB in Spring Run 1 (Table 3, Fig. 6). No CSRB were found in the Upper Spring Run, which was dropped from analyses, including from MIPU analyses to maintain equivalent comparisons between species.

Table 3. Total number of samples and larval and adult CSRB and MIPU found during the study, excluding all lures that were dry or disturbed.

Locality	Samples	CSRB larvae	CSRB adults	MIPU larvae	MIPU adults
Spring Island	90	93	402	56	330
Spring Run 1	39	0	1	6	5
Spring Run 3	87	27	126	12	154
Upper Spring Run	48	0	0	109	96
Western Shoreline	89	76	101	37	98
Total	353	196	630	220	683

Trends in mean abundance of both life stages of CSRB and MIPU did not show any clear temporal variation in abundance that could be indicative of phenological differences in abundance by season (Appendix Figs. S6–S9). For a thermally stable spring system and a species (CSRB) that primarily occurs in dark microhabitats, it is not surprising to find no phenological variation with season, but this narrow thermal tolerance could threaten the species if conditions were to change (Cooke et al. 2015, Polášková et al. 2022).

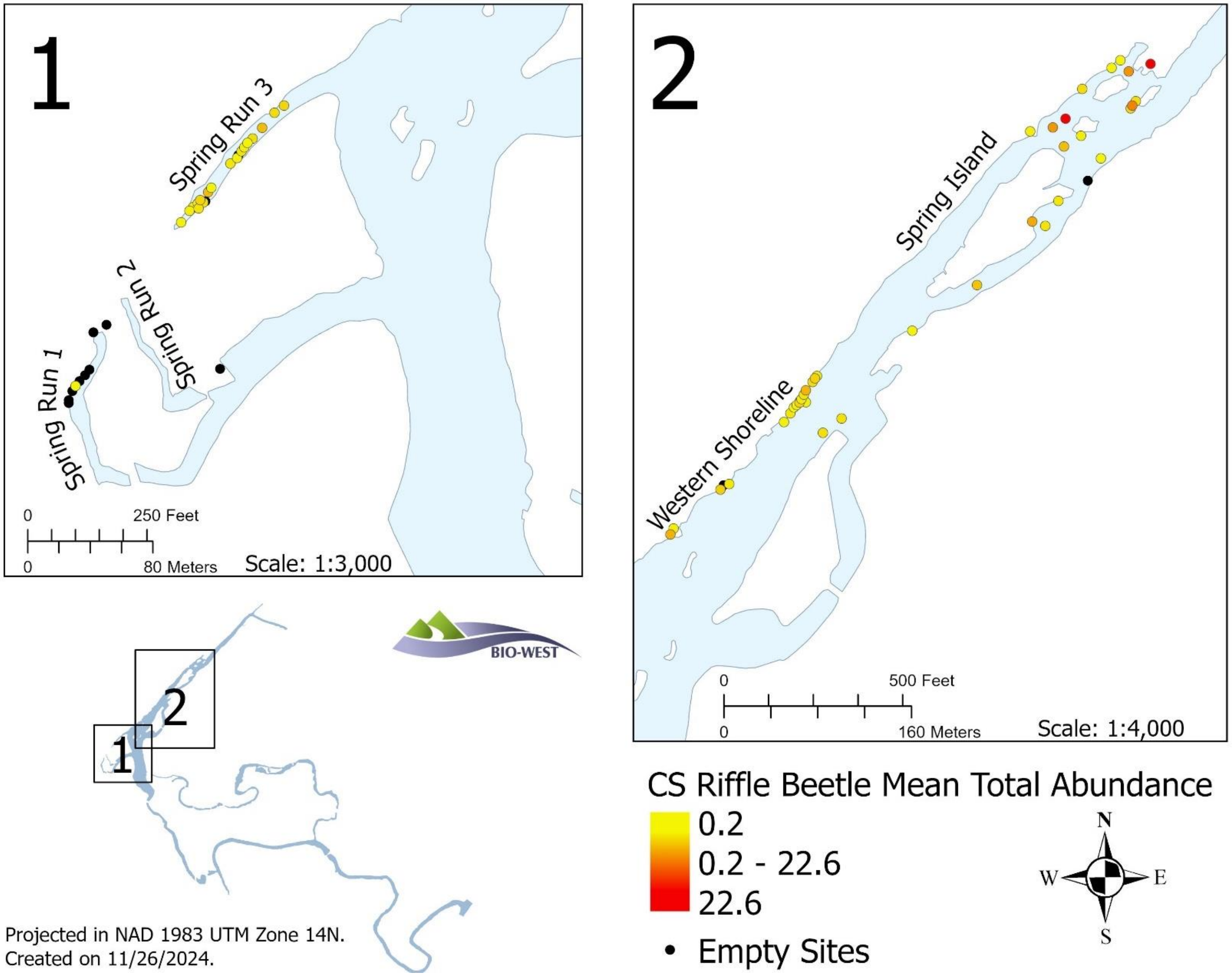

Figure 6. Locations where any individuals either CSRB life stage were observed (empty sites = no CSRB found) and mean total (adults + larvae) CSRB per lure across the duration of the study.

4.1b Covariates

Water quality variables showed little variation across the study and no clear relationships with beetle abundance, as was expected in a stable spring system (Appendix Figs. S10–S12). Some upwelling sites, particularly around Spring Island, exhibited higher dissolved oxygen levels (Appendix Fig. S10), which was likely related to their proximity to aquatic vegetation. At these sites and the microhabitats beetles occupied, obtaining accurate dissolved oxygen measurements of water flowing from the aquifer with a probe that was much larger than the spring openings was nearly impossible.

Conductivity dropped slightly when it rained prior to measurements, but still showed generally little variation across the system (Appendix Fig. S11). Lures were set at depths from just below the water surface (~2 cm) to over 2 m deep (Fig. S13), and CSRB and MIPU were found at sites across those ranges of depths. Substrate varied from sites that were nearly all boulder/bedrock to those that were all silt/sand (Appendix Fig. S14); beetles were found at sites across the range of substrate sizes. While preliminary analyses suggested that higher numbers of beetles may be found in smaller substrate sizes (Fig. 7), this was tied to higher CSRB abundances and smaller substrate sizes at Spring Island sites, which were the most stable (consistently under water and stable springflow) throughout the study.

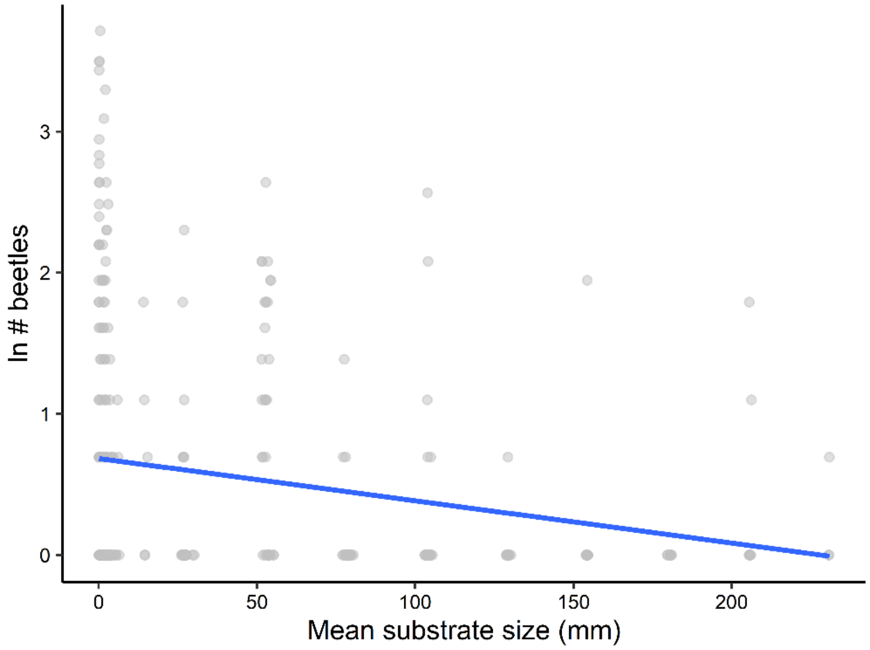

Figure 7. Initial comparison between natural log-transformed adult CSRB abundances and mean substrate size suggested an inverse relationship between the two.

Site-level springflow varied by site and locality across the five sampling periods (Fig. 8), however, there was no clear relationship between site-level springflow and beetle abundance (Appendix Fig. S15). Lures were always set in flowing springs, and beetles were found across the range of site-level flows observed. Initial analyses suggested a possible relationship between total system springflow and beetle abundance, and this was refined into a calculation of local spring flow described in section 4.2. Local springflow also accounted for potential effects of spatial group factors observed in initial data exploration.

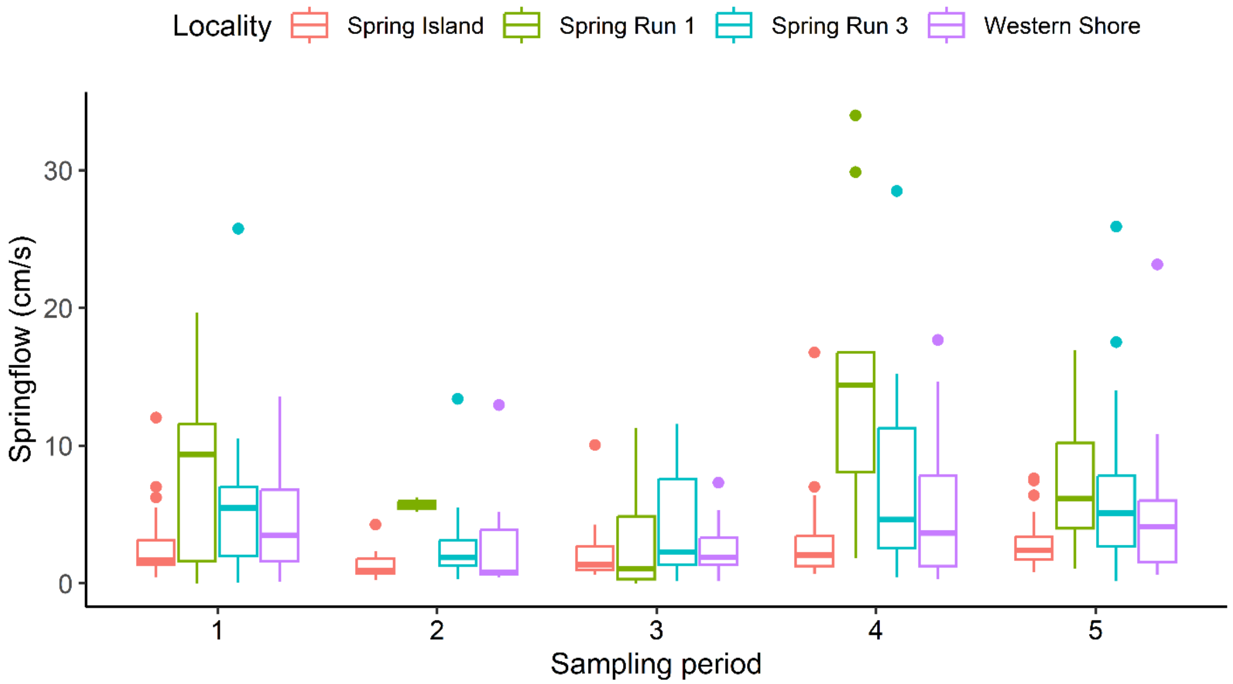

Figure 8. Boxplots of average site-level springflow (mean of starting and ending measurements) set by locality and sampling period.

There was no clear effect of the presence of any organic matter type in the spring area on the abundance of beetles (Appendix Fig. S16). At Spring Island, abundances of both life stages appeared higher when roots were absent, but this pattern was not consistent across other localities. Also at Spring Island, adult abundance trended higher and larval abundance lower when wood was present, but this trend was again not consistent across other localities. Even if beetles are attracted to organic material, any organic material on the spring surface may have no effect on near-surface beetle populations, while organic material deeper within springs that was undetected could have an effect on beetle populations. Organic material presence was excluded from subsequent analyses.

Estimated biofilm coverage on the lures varied widely among samples with no clear temporal or spatial patterns (Appendix Fig. S17). However, initial comparisons suggested a potential positive relationship between biofilm coverage and CSRB abundance (Fig. 9). Biofilm coverage and local springflow were the two covariates included in final analyses (see section 4.3).

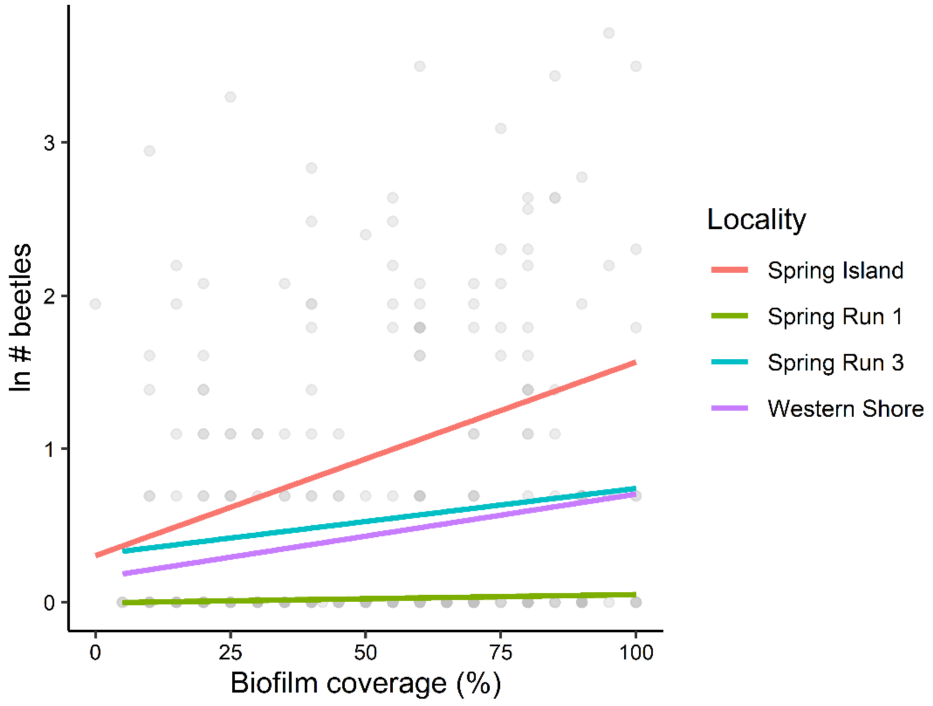

Figure 9. Scatterplot of natural log-transformed adult CSRB abundance and percent biofilm coverage on lures across the four sampling localities.

4.2 Local springflow

From 2003–2024, discharge across the eight monitoring stations ranged from 0–166 cfs (mean = 26 cfs) and mean daily total system springflow ranged from 55–446 cfs (mean = 200 cfs). Long-term (1938–2024) average for total system springflow was 280 cfs. Performance metrics demonstrated the fitted LMM explained a large proportion of variation in the response (conditional R^2 = 0.99), was able to predict training data with high accuracy (RMSE = 3.66 cfs), and generalized to out-of-sample data ($RMSE_{cv}$ = 3.80 ± 0.26) (Table 4). Functional relationships for local discharge at each station are shown in Fig. 10.

Table 4. Summary of parameter estimates, standard errors (SE), and performance metrics for the linear mixed effects model used to predict station-level discharge.

Parameters	Estimate	SE
Fixed effects coefficients		
Intercept	44.59	12.73
Mean-daily total system springflow	0.17	0.04
Random effects standard deviation		
Station intercepts	35.99	-
Station slopes	0.11	-
Predictive Performance		
$R^2_{conditional}$	0.99	-
Residual standard deviation	3.74	-
RMSE	3.66	-
$RMSE_{cv}$	3.80	0.26

Good performance displayed by the LMM supports that it is a reliable quantitative tool for characterizing local springflow conditions at each CSRB study site. This is further illustrated in Fig. 11, which displays a predicted time-series of local springflow at each station from 2001–2024 and demonstrates their agreement with empirical measurements conducted from 2003–2024. Therefore, 30-day local springflow average was calculated on the date of lure retrieval and included as a GLMM covariate (Table 5).

Table 5. Summary statistics for 30-day local springflow average (cfs) during the study duration (April 2023–May 2024) for discharge stations linked to each site.

Site	Station	Mean	Minimum	Maximum
Spring Island	Spring Island Lower Near	16.13	7.11	22.95
Spring Island	Spring Island Upper Far	22.94	13.63	31.02
Western Shoreline	Total Springflow - Landa Lake Cable	75.37	42.45	101.74
Spring Run 3	Spring Run 3	14.38	6.57	20.60
Spring Run 1	Spring Run 1	7.54	0.34	13.03

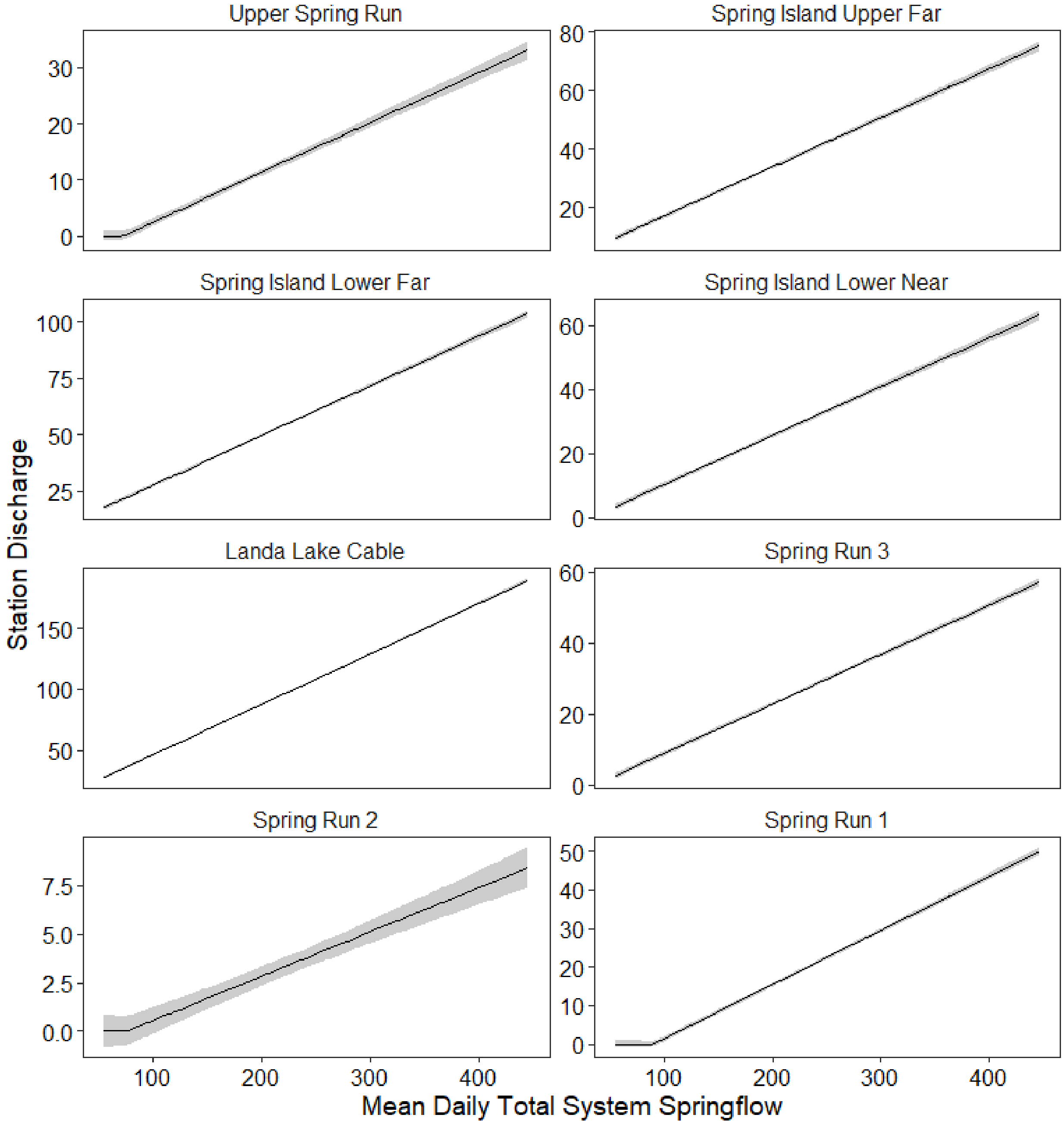

Figure 10. Fitted predictions of discharge (cfs) as a function of mean daily total system springflow (cfs) across at eight stations in Comal Springs. Solid lines and grey polygons represent the line-of-best-fit and ±1 standard error, respectively.

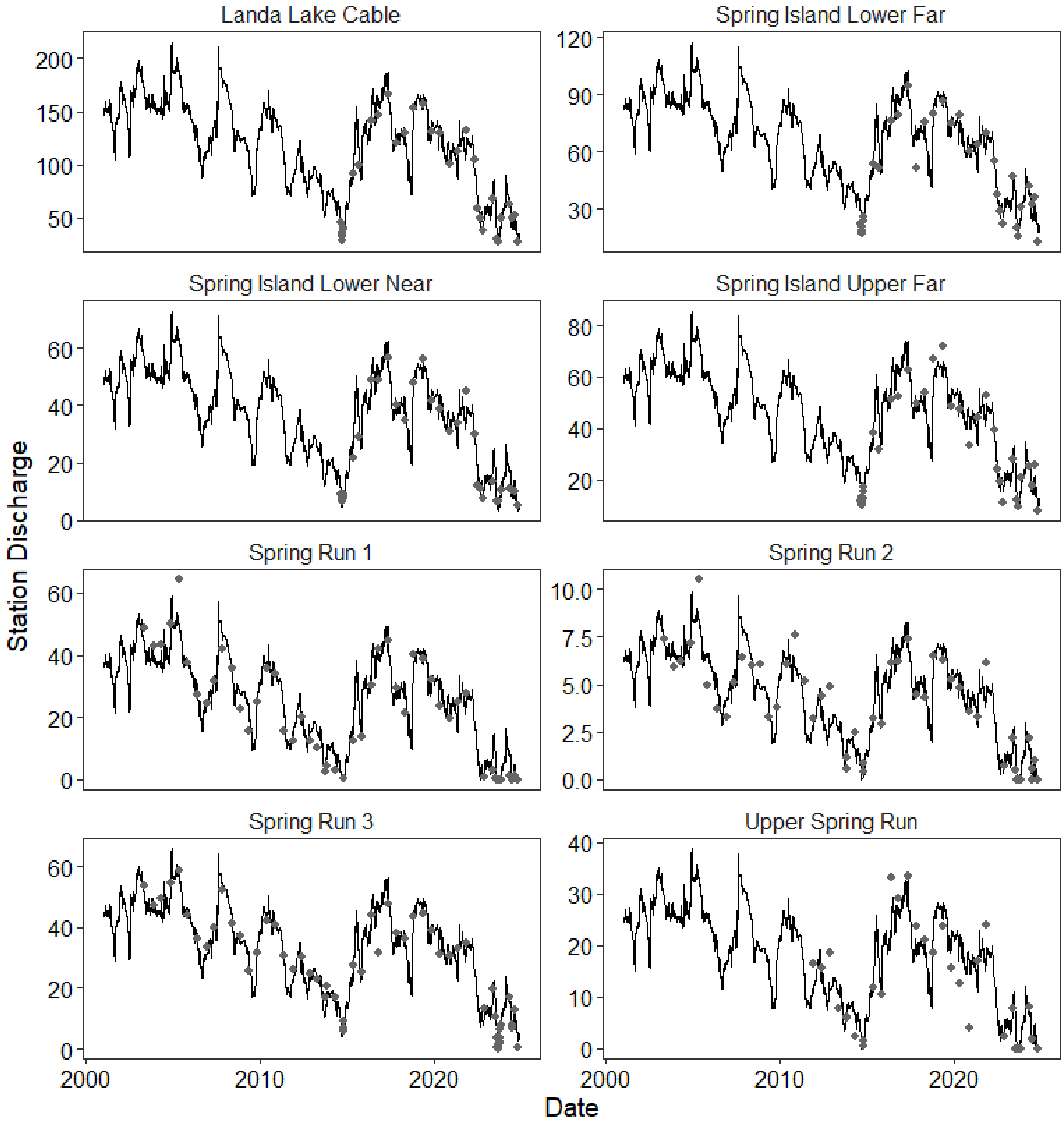

Figure 11. Local springflow time-series from 2001–2024 at eight stations discharge measurement stations in Comal Springs. Solid lines represent LMM predictions per station and grey data points denote observed discharge measurements from 2003–2024.

4.3 Relative abundance

4.3a Model evaluation

All GLMMs converged with trace plots showing adequate mixtures of MCMC chains and $\check{R}$ less than 1.1 for all parameters monitored. Density plots of marginal posterior distributions also aligned among MCMC chains. Results from all goodness-of-fit assessments revealed adequate fit between model estimates and observed data. Marginal R^2 represents the variation explained by the site-level intercepts and slopes and estimates ranged from 0.64–0.85. Conditional R^2 includes the added variation explained by random effects, which ranged from 0.61–0.93 and explained 0.51–0.62 more variance than marginal R^2. This indicated the random effects components explained a relatively greater amount of variation in relative abundance. Overlap in R^2 90 % BCIs also illustrated uncertainty in differences in proportion of variation explained between GLMMs (Table 6).

Table 6. Estimates (90 % Bayesian credible interval) of performance statistics used to evaluate the goodness-of-fit for generalized linear mixed effects models of relative abundance.

Statistic	CSRB Adults	CSRB Larvae	MIPU Adults	MIPU Larvae
Variation explained				
$R^2_{marginal}$	0.19 (0.06 - 0.39)	0.13 (0.04 - 0.32)	0.18 (0.06 - 0.37)	0.33 (0.14 - 0.57)
$R^2_{conditional}$	0.81 (0.49 - 0.95)	0.64 (0.21 - 0.93)	0.79 (0.47 - 0.94)	0.85 (0.64 - 0.94)
Posterior predictive checks				
B_p (χ^2 discrepancy)	0.45	0.52	0.50	0.51
$RMSE_{obs}$	1.27 (1.07 - 1.52)	0.85 (0.72 - 1.02)	1.27 (1.08 - 1.53)	0.61 (0.49 - 0.76)
$RMSE_{sim}$	1.26 (1.06 - 1.54)	0.84 (0.70 - 1.03)	1.27 (1.07 - 1.54)	0.61 (0.48 - 0.77)
Cross-validation				
$RMSE_{cv}$	4.11	8.90	4.50	1.33

Posterior predictive checks illustrated GLMMs were reasonable descriptions of the observed data. Bayesian *p*-values ranged from 0.45–0.52 and supports that data simulated by each model were consistent with observed data. This was further demonstrated by similar observed and simulated RMSE estimates for each model. Relatively low estimates of RMSE (0.61–1.27) illustrated by posterior predictive checks also supports that the GLMMs predicted relative abundance with good accuracy. That said, cross-validation RMSE was substantially higher relative to posterior predictive checks, ranging from 1.33–8.90. Compared to other RMSE estimates, cross-validation RMSE was about 1.2 times higher for MIPU larvae, 2.5 times higher for CSRB and MIPU adults, and 9.6 times higher for CSRB larvae. Differences in predictive accuracy between these two evaluation procedures indicated some uncertainty in each model's ability to generalize to new data (Table 6).

4.3b Parameter estimates and functional relationships

Average relative abundances represent site-level intercepts on the original response scale (counts/lure), which were used to derive apparent occupancy probability (Table 7). Differences in intercept estimates on the relative abundance scale are described here and apparent occupancy between sites are included in Fig. 12 for comparison. Intercept estimates were zero at Spring Run 1 for each species-life stage combination and was also zero for MIPU larvae at Spring Run 3. Site-level intercept estimates (90% BCI) for CSRB adults were 0.52 (0.32–0.81) at Spring Island, 0.07 (0.03–0.14) at Western Shoreline, and 0.11 (0.06–0.18) at Spring Run 3. Credible intervals for Spring Island did not overlap with other sites, suggesting it is highly probable that average relative abundance was greater at this site relative to others. Intercepts for CSRB larvae, MIPU adults, and MIPU larvae also illustrated greater average relative abundance at Spring Island. However, broad and overlapping credible intervals indicated uncertainty in whether average relative abundance truly differed between sites (Fig. 12).

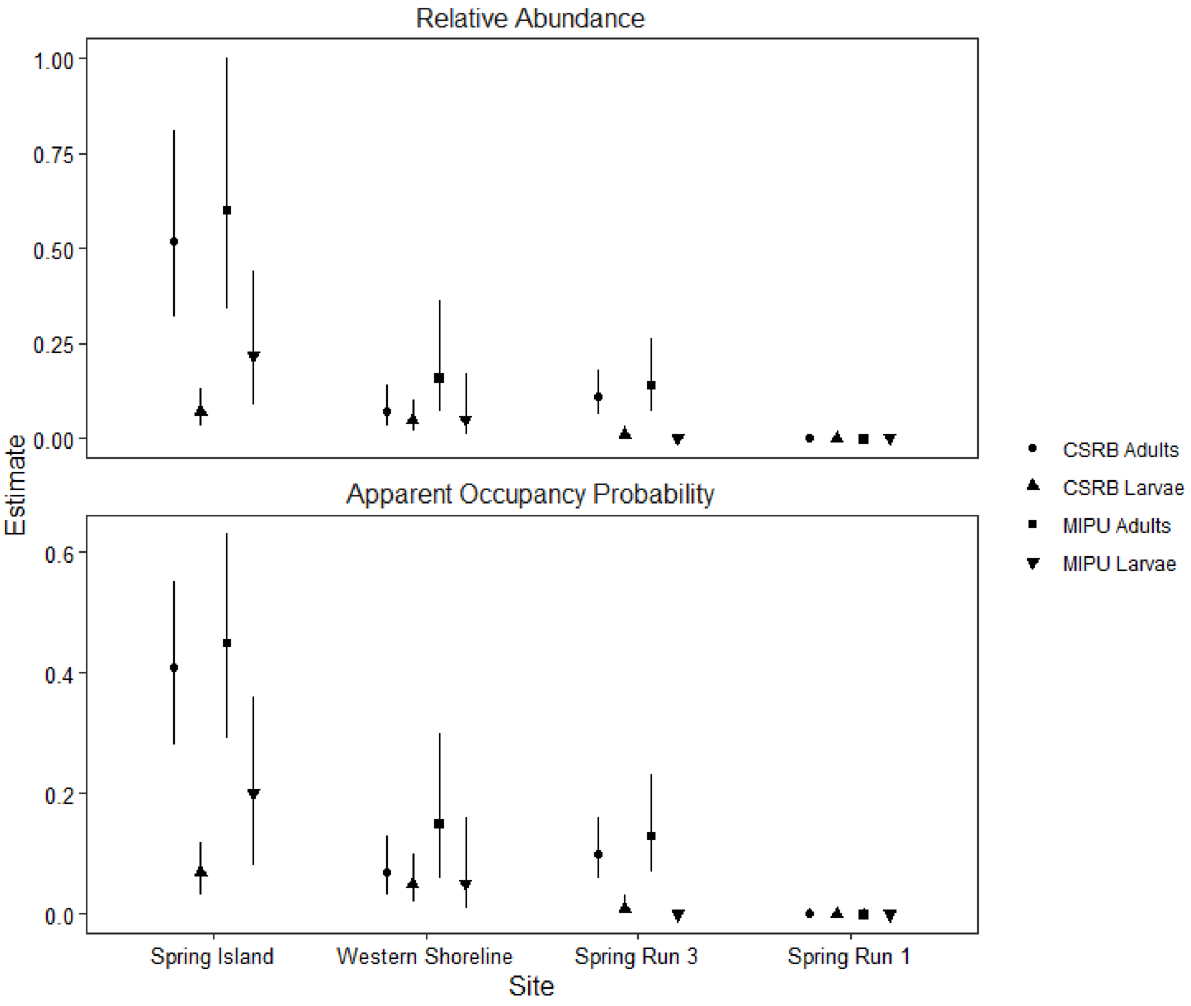

Figure 12. Generalized linear mixed effects model estimates of average relative abundance and apparent occupancy probability at each site. Average relative abundances represent site-level intercepts on the original response scale (counts/lure), which were used to derive apparent occupancy probability. Error bars denote 90 % Bayesian credible intervals.

Table 7. Estimates (Est) and Bayesian credible intervals (BCI) of parameters used to fit generalized linear mixed effects model of relative abundance.

	CSRB Adults		**CSRB Larvae**		**MIPU Adults**		**MIPU Larvae**	
Parameter	**Est**	**BCI**	**Est**	**BCI**	**Est**	**BCI**	**Est**	**BCI**
Intercepts								
Spring Island	-0.65	(-1.13 - -0.22)	-2.68	(-3.44 - -2.04)	-0.50	(-1.08 - 0.00)	-1.52	(-2.44 - -0.81)
Western Shoreline	-2.68	(-3.43 - -2.00)	-3.03	(-3.89 - -2.28)	-1.81	(-2.72 - -1.02)	-2.94	(-4.49 - -1.75)
Spring Run 3	-2.22	(-2.76 - -1.72)	-4.38	(-5.39 - -3.53)	-1.98	(-2.68 - -1.37)	-11.26	(-22.92 - -6.57)
Spring Run 1	-7.62	(-16.57 - -4.59)	-7.06	(-15.44 - -4.38)	-8.01	(-17.02 - -4.79)	-10.70	(-22.55 - -5.81)
Population-level intercept	-3.29	(-8.49 - 0.62)	-4.25	(-8.75 - -1.29)	-3.07	(-8.54 - 1.04)	-6.78	(-14.37 - -1.35)
Covariate Effect Size								
30-day local springflow average	0.14	(0.06 - 0.21)	0.30	(0.22 - 0.40)	0.03	(-0.06 - 0.12)	-0.13	(-0.29 - 0.02)
Percent total biofilm	0.04	(0.03 - 0.05)	0.03	(0.02 - 0.05)	0.01	(0.00 - 0.03)	0.00	(-0.02 - 0.02)
Random effects standard deviation								
Site	4.32	(1.65 - 9.09)	3.01	(0.94 - 8.47)	4.67	(1.84 - 9.17)	6.56	(2.93 - 9.64)
Extra-residual	1.55	(1.33 - 1.82)	1.56	(1.28 - 1.9)	2.02	(1.75 - 2.35)	2.25	(1.75 - 2.98)

For each GLMM, random effects standard deviations were higher for site compared to the extra-residual term. This indicated there were larger differences in relative abundance between sites that weren't accounted for by the model covariates relative to the observation-level. Estimates (90% BCI) of 30-day local springflow average effect size for each CSRB life stage was 0.14 (0.06–0.21) for adults and 0.30 (0.22–0.40) for larvae. Slope estimates for effect size of total biofilm on CSRB relative abundance was 0.04 (0.03–0.05) for adults and 0.03 (0.02–0.05) for juveniles. Bayesian credible intervals for CSRB adult and larvae slopes did not overlap with zero, meaning there was a 0.9 probability that both covariates had a positive non-zero effect on relative abundance. For MIPU, local springflow and total biofilm effect sizes were 0.03 (-0.06–0.12) and 0.01 (0.00–0.03) for adults and -0.13 (-0.29–0.02) and 0.00 (-0.02–0.02) for juveniles, respectively. In contrast to CSRB, the breadth of BCIs for both MIPU life stages failed to reject zero as a plausible effect size by each covariate (Table 7).

Relationships of CSRB relative abundance and apparent occupancy probability are presented for adults and larvae in Fig. 13. Extent of 30-day local springflow averages on the x-axis of each panel encompass the range of discharge magnitudes observed at each site over the study period. Since the effect size of local springflow was fixed across sites, maximum predictions of relative abundance and apparent occupancy probability occurred at Spring Island and Western Shoreline because they exhibited the greatest maximum 30-day local springflow averages. Consequently, as local springflow decreased from its maximum to minimum magnitude, state variables for both life stages were expected to decrease by about 90–100% at Spring Island and Western Shoreline. At Spring Run 3 in contrast, CSRB adult state variables were expected to decrease by about 85% compared to an expected decline near 100% for CSRB larvae. It is also important to note that relative abundance predictions for CSRB larvae at Western Shoreline showed an exponential increase from about 1–139 counts/lure as local springflow increased from 85–100 cfs. Maximum predictions of CSRB larvae at this site were much higher than the observed maximum (14 counts/lure), suggesting the slope estimate of local springflow was not realistic for this life stage (Fig. 13).

Given that total biofilm was quantified as a percentage, its functional relationship with CSRB adults and larvae were more consistent between sites relative to local springflow. Differences in maximum predictions were therefore governed by estimates of each site's intercept. As total biofilm increased from 0–100%, relative abundance and apparent occupancy probability were expected to increase about 97% for both life stages. Lastly, predicted values of relative abundance and apparent occupancy were very similar for all fitted functions except CSRB adults at Spring Island, which illustrated that as relative abundance approached 3.0 counts/lure, apparent occupancy probability approached 1.0 (Fig. 14).

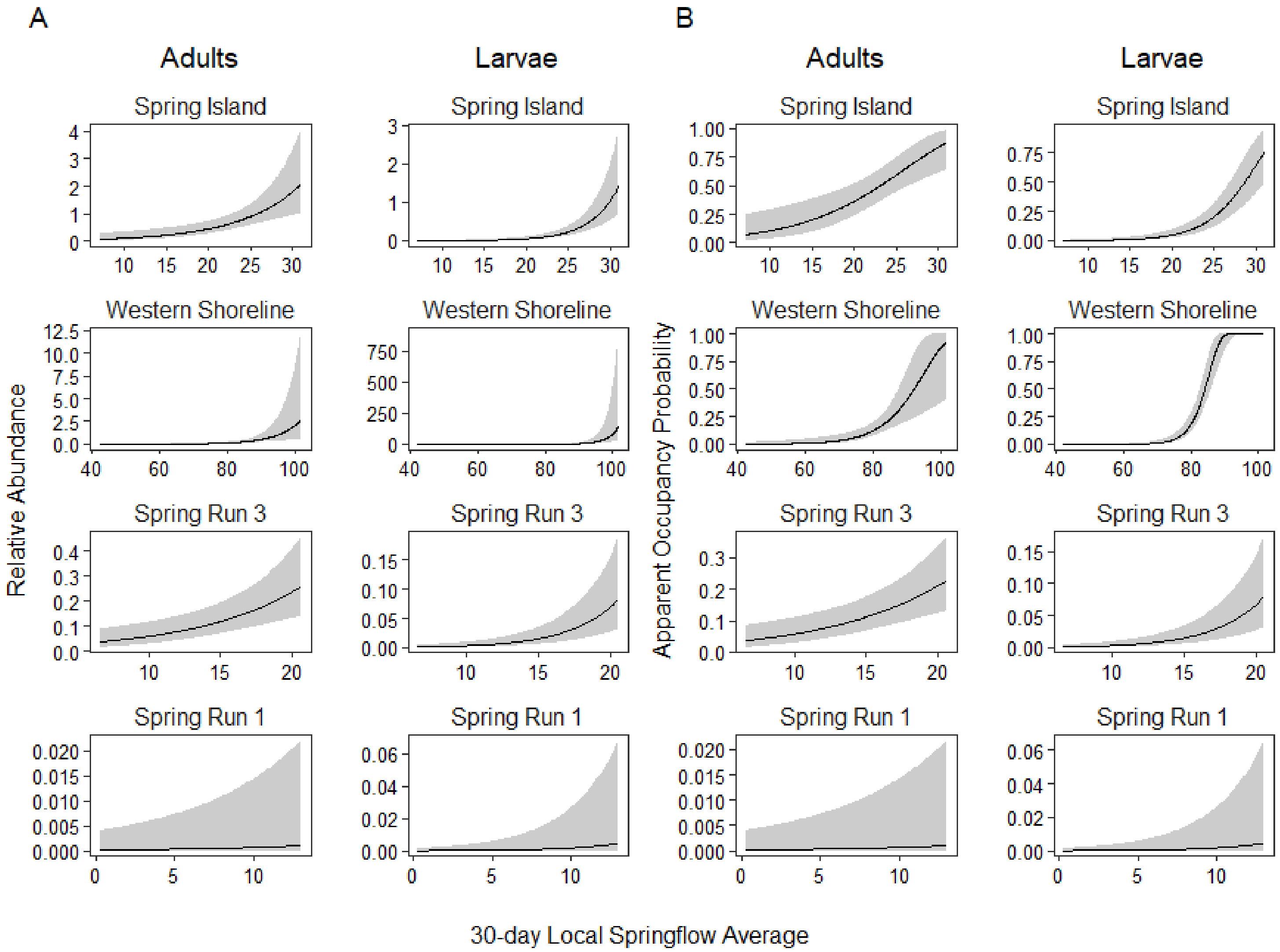

Figure 13. Relative abundance (A) and apparent occupancy probability (B) relationships with **30-day local springflow** average among sites for CSRB adults and larvae. Solid lines represent mean relative abundance predictions by the posterior distributions of each parameter and solid polygons denote 90 % Bayesian credible intervals.

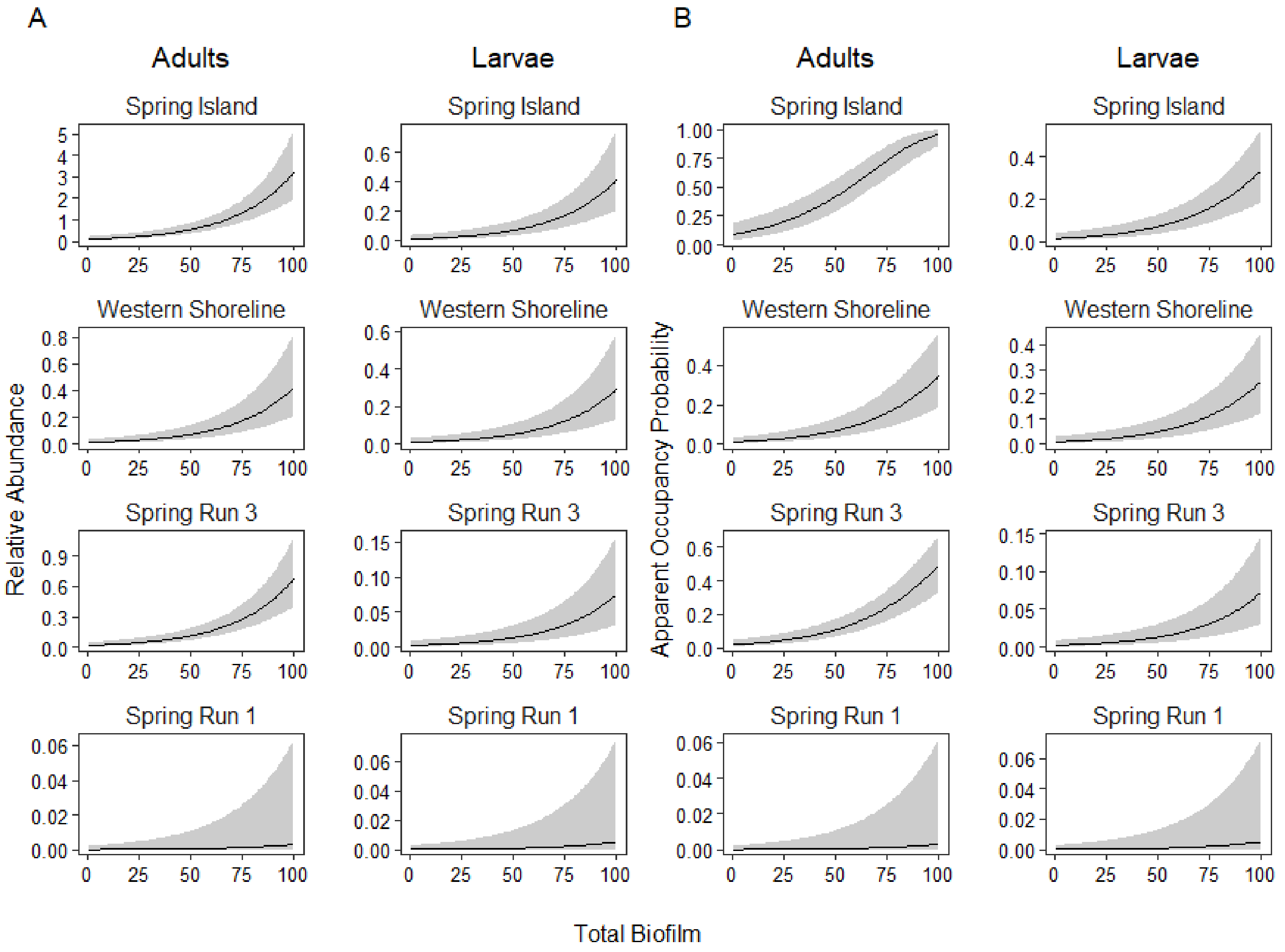

Figure 14. Relative abundance (A) and apparent occupancy probability (B) relationships with **total biofilm** average among sites for CSRB adults and larvae. Solid lines represent mean relative abundance predictions by the posterior distributions of each parameter and solid polygons denote 90 % Bayesian credible intervals.

4.3c Framework for biological monitoring applications

In fall 2024, 30-day local springflow average was 4.4–10.7 cfs at Spring Island, 31.0 cfs at Western Shoreline, and 3.7 cfs at Spring Run 3. Total biofilm across sites ranged from 10–85%. CSRB were only detected at 10% of lure samples (n = 3 lures). Observed CSRB relative abundance across sites ranged from 0–26 counts/lure (median = 0.00 counts/lure) and the GLMM's overall posterior forecast distribution ranged from 0.00–8.17 counts/lure (median = 0.01 counts/lure). Estimated RMSE was 4.79 (4.75–4.80), indicating relatively low predictive accuracy. That said, given that 90% of the observed data were zeros, it was not surprising that this global measurement of accuracy was poor, and suggests estimated RMSE was likely strongly influenced by the one sample with high relative abundance (26 counts/lure). Residual diagnostics, which examine model accuracy more locally, instead exemplified that residuals were centered around zero and displayed no strong patterns. This alternatively suggests adequate model fit and that the larger predictive errors represented stochastic variation (Fig. 15).

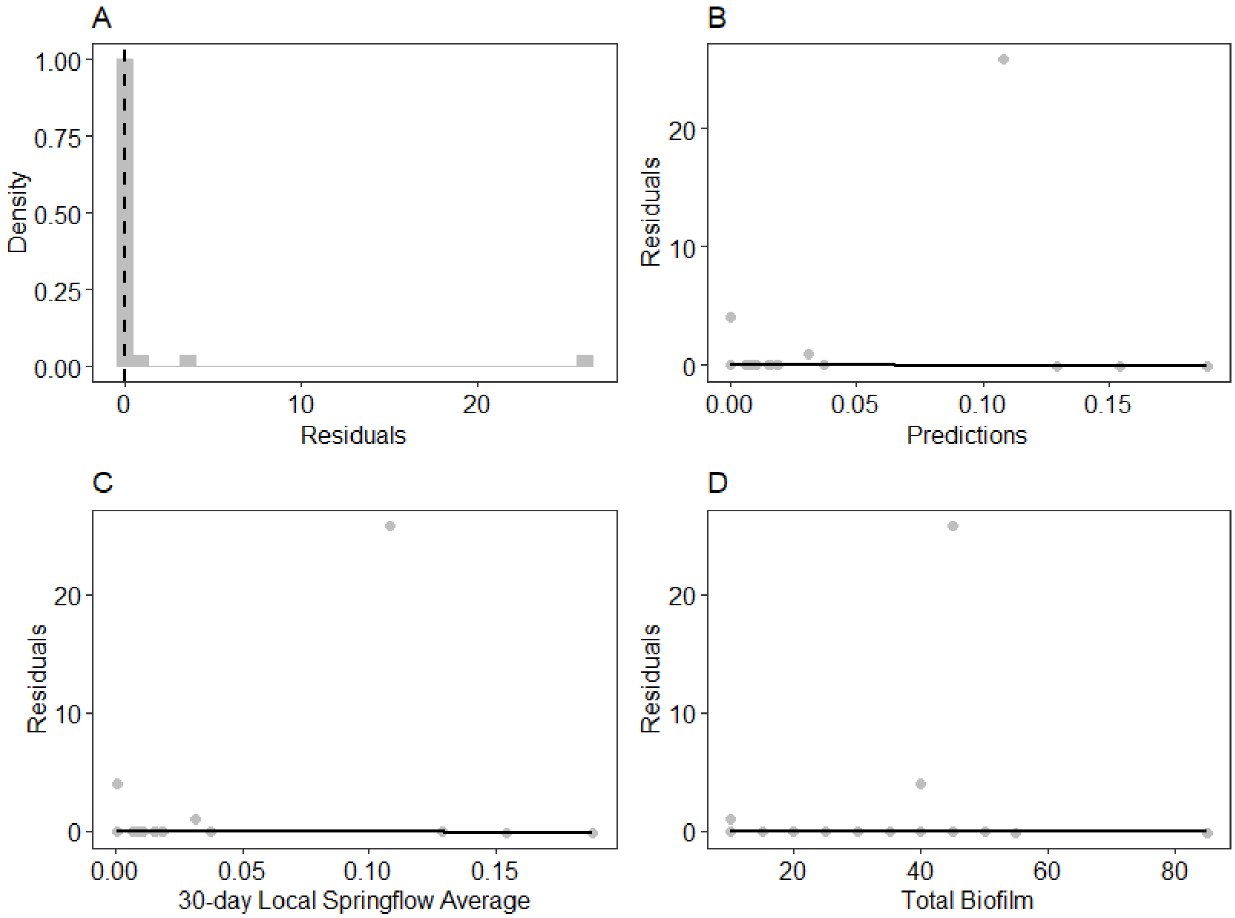

Figure 15. Diagnostic plots for residuals of the generalized linear mixed effects model used to forecast CSRB adult relative abundance during the fall 2024 EAHCP biological monitoring event. Plots include a histogram of residuals (A) and scatterplots of residuals versus predictions (B), 30-day local springflow average (C), and total biofilm (D). The black line fit to scatterplots on panel B–D represent quantile regression line-of-best-fit (quantile = 0.5).

Among sites, observed median relative abundance was 0.00 counts/lure, which closely aligned with expectations predicted by the GLMM. Expected relative abundance was also 0.00 counts/lure at Western Shoreline. At Spring Run 3, the expectation was 0.01 and its 90% BCI (0.00–0.04) included zero. Spring Island observations were slightly lower than expectations, but still approximated the predicted value of 0.07 (0.01–0.35) (Table 8). Boxplots shown in Fig. 16 further demonstrated that posterior forecast distributions only include lower predictions of relative abundance near 0.00 counts/lure for each site.

Table 8. Summary of observed and expected (90% BCI) median relative abundance of CSRB adults during the fall 2024 EAHCP biological monitoring event.

	Median Relative Abundance	
Site	**Observed (Fall 20224)**	**Expected**
Spring Island	0.00	0.07 (0.01-0.35)
Western Shoreline	0.00	0.00 (0.00-0.00)
Spring Run 3	0.00	0.01 (0.01-0.04)

Given that observations approximated expectations predicted by the GLMM, this would lead to the conclusion that patterns of CSRB relative abundance in fall 2024 were likely attributed to covariate effects. This provides evidence to suggest very low relative abundances in fall 2024 were best explained by the extreme low flow conditions experienced in Comal Springs during this time period (55–74 cfs). Underestimates of several lure samples could be due to a variety of stochastic factors that are currently unknown.

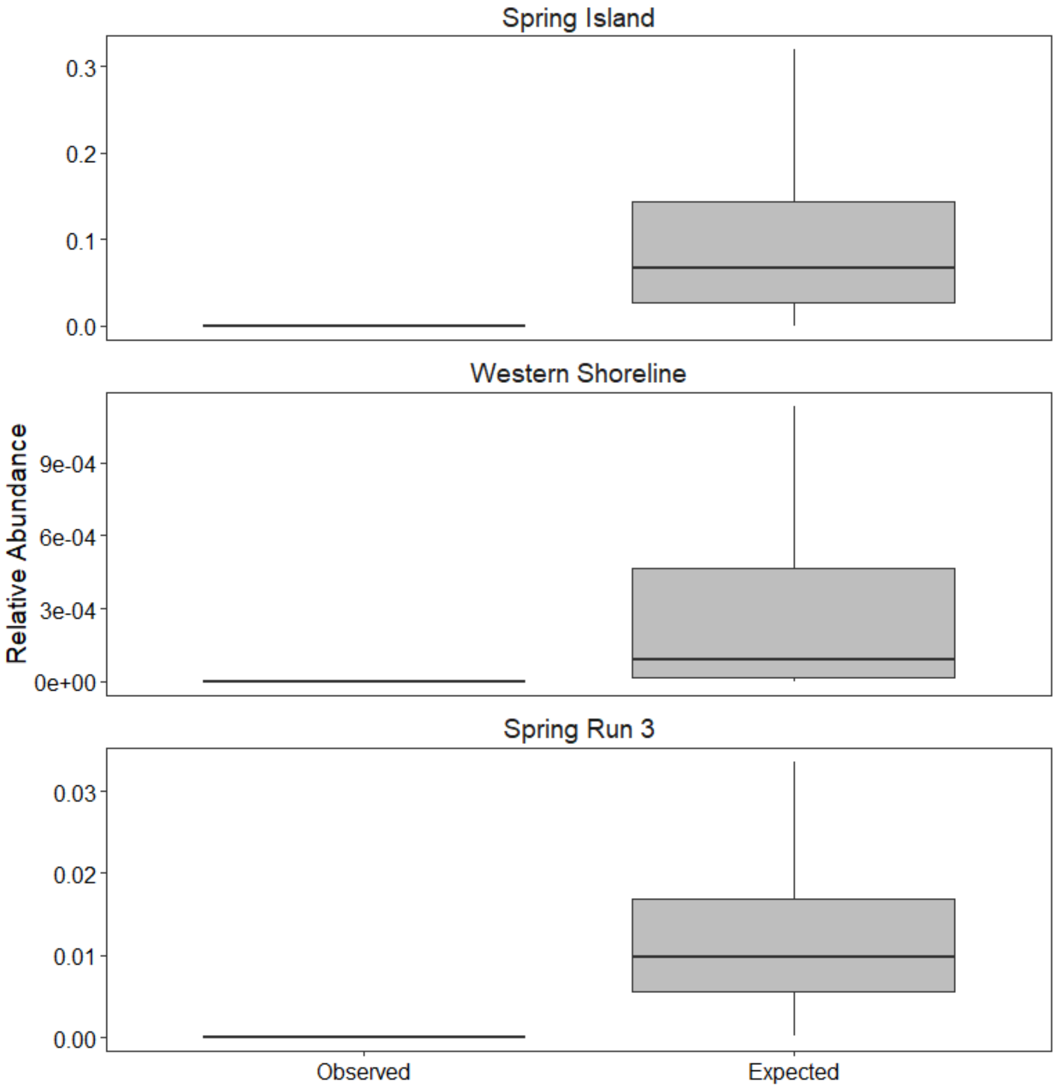

Figure 16. Boxplots comparing CSRB adult relative abundances observed in fall 2024 versus expected values predicted by the generalized linear mixed effects model. The thick horizontal line in each box is the median and the upper and lower bounds of each box represents the interquartile range. Whiskers represent minimum and maximum values up to 1.5 times the interquartile range

5. Discussion

5.1 CSRB spatial and temporal distribution

CSRB were found at least once at nearly all sites in Spring Run 3, Western Shoreline, and Spring Island, but there was only a single occurrence in Spring Run 1 and none in the Upper Spring Run. The highest recorded abundances were around Spring Island, which generally had the most stable habitats that were consistently underwater and maintained springflow throughout the drought. In particular, the upwelling sites northeast of Spring Island reliably supported the highest numbers of CSRB throughout the study (Fig. 6). The lower abundances in Spring Run 3 and Western Shoreline may be a combination of these areas generally supporting fewer CSRB and the effects of drought. Most sites in Spring Run 3 and the Western Shoreline were terrestrial margin habitats that had water levels drop or ceased detectible flow during low-flow periods. Similarly, the lack of CSRB occurrence in Spring Run 1 is possibly a reflection of the ongoing drought that began in 2022 that led to the upper portions of Spring Run 1 completely drying in summer 2023 (and again in late 2024).

There has been only one reported CSRB occurrence from the Upper Spring Run, and our study, combined with prior surveys in the locality, suggest that the area does not support a CSRB subpopulation. Although most of our sites in the Upper Spring Run did not dry at all during the study (five sites were >1 m deep), overall flows were noticeably reduced at all of the sites during summer and fall sampling. Only a single individual of a spring-endemic species was found (*Stygobromus* sp.) in the Upper Spring Run during our study. Conversely, MIPU were found at half of the sites in the Upper Spring Run. Multiple reliable records of *S. comalensis* have been reported from the Upper Spring Run, and this species contrasts with CSRB in that it likely utilizes subterranean habitats. Therefore, *S*. *comalensis* may be able connect to other areas of the Comal Springs system through subterranean passages and recolonize the near-surface sites in the Upper Spring Run when conditions are favorable.

CSRB were found on lures at the entire range of depths that we sampled at, from the deepest site (>2 m) to lures at the water surface. Occurrence of CSRB on lures at or just above the water surface only happened when lures were still wet. This was likely a reflection of a recent drop in water levels in the time since they were set that left beetles that had previously colonized the lures stranded within them; completely dry lures never had CSRB. Our lures were only placed in favorable locations at the time they were set: just below the substrate – water interface where there was noticeable flow. Initial tests of layering lures at different depths largely only found CSRB at the substrate – water surface interface (BIO-WEST unpublished data). The sum of evidence to date suggests that CSRB predominantly occur in these microhabitats, and we hypothesize that there is unlikely a true subsurface population as there probably is with the other endemic spring-associated invertebrates (*S. comalensis*, *Stygobromus* spp.).

While visual examination of the data suggests that there might have been some slight locality-specific changes in mean CSRB adult and larval abundances over time in the study (Appendix Figs. S6–S7), there were no consistent patterns. If CSRB had a clear seasonal phenology, we would have expected to see consistently higher/lower abundances of adults and/or larvae during certain sampling periods. The initial suggestion by Bowles et al. (2003) that CSRB larvae may be more abundant during fall may have actually been differences in abundance related to an environmental factor not accounted for at the time of their study. Additionally, our results suggest that cotton lures are not as reliable at detecting the presence and assessing the abundance of CSRB larvae as they are for adults (see section 5.2).

It has long been suggested that CSRB are negatively impacted by silt or other fine sediments (NAS 2018; USFWS 2024), but there has been a lack of data or direct assessment of this factor. This idea likely originated from observations that lures that experienced noticeable sedimentation as a result of sediment being washed down onto lures and springs from the above terrestrial habitats following significant rainfall events. Only one of our lures experienced significant sedimentation to the extent that it noticeably impacted the quality of the lure, and this was at a site under the rock wall in Spring Run 1 during summer 2023 that partially caved in from above as the spring run dried. Other sites commonly had sediment on top, and lures were placed in sites surrounded by fine sediments (and some entirely in sand and silt). We found no evidence in this study or other recent work (BIO-WEST 2025) that suggests the presence of silt within spring sites has any negative effect on CSRB abundance. It appears that as long as spring sites maintain flow, there is no noticeable effect on CSRB.

5.2 Model results and covariate effects

Our model results indicated that both CSRB adults and larvae responded positively to local springflow and lure biofilm coverage but that other site characteristics did not affect relative abundance. For both CSRB life stages, local springflow had a larger effect than biofilm coverage. The lack of effect of other covariates on CSRB relative abundance support the limited work of previous studies, which also found no effect of various covariates (Bowles et al. 2003). However, while we found that site-level springflow (measured at each lure) had no effect, our calculated measure of local springflow did. This is perhaps suggestive that local springflow is a better indication of local habitat quality and stability, and it reflects conditions that affect entire subpopulations rather than an individual site. Local springflow also characterized average conditions across the entire sampling period lures were set, while site-level springflow was an average of two point-measurements (start, end). Individual sites have more variable site-level counts of beetles than overall localities, potentially owing to imperfect detection or other stochastic processes. While not a perfect indicator of locality-level conditions, when local springflow is modeled within each locality, unique locality-specific relationships are generated that further reflect the stability of the springflow and favorable CSRB habitat in each locality.

The small positive relationship of CSRB relative abundance with biofilm likely reflects the response of CSRB to greater availability of this food resource. This relationship should be expected, but it is perhaps somewhat surprising that this covariate was the only sample-level covariate included in our final model. The causes of variation in biofilm coverage of lures remain unknown, but we expect that it is tied to some other unmeasured characteristic of each site and the site-level processes that inoculated and supported the growth of biofilm on lures. Our estimates of biofilm coverage were obtained by a single person and theoretically were as consistent as possible across the duration of the study. Variation in estimates should be expected if different observers were to estimate coverage. However, because of the relatively small effect of biofilm and potential inaccuracy with variation in observer estimates over time, we explored alternate model formulations that excluded biofilm. These alternate model results performed similarly (Appendix Table S1) and indicated that excluding biofilm from models may be sufficient for assessing the status of CSRB populations over time (see section 5.3) without potential observer-level variation in biofilm estimates.

Marginal and conditional R^2 values for CSRB larvae trended lower than for adults, but all 90% BCIs overlapped (Table 6). This may reflect that while CSRB larval relative abundance was affected by our covariates, the cotton lure methodology is not as effective at assessing relative abundance of CSRB larvae as it is for adults. This also supported by the relative abundance and occupancy estimates for larvae, which were consistently lower with overlapping BCIs for Spring Island, Western Shoreline, and Spring Run 3. This is in contrast to CSRB adults, which had higher relative abundance and occupancy estimates at Spring Island than other localities. We would expect true abundance and occupancy of adults and larvae to be correlated – areas with more adults should also have more larvae. Preliminary results using an alternative sampling method (wood discs), indicated that there was similar abundance of CSRB larvae and adults on wood discs, but much lower abundances of larvae than adults on cotton lures (BIO-WEST 2025), further supporting the supposition that cotton lures are not as effective for assessing CSRB larvae.

The effects of local springflow and biofilm on CSRB contrasts with MIPU, for which all covariate BCIs overlapped with zero (Table 7), rejecting a plausible non-zero effect of both covariates on that species. However, the effect of springflow on MIPU larvae trended towards a negative effect, and further investigation focused on MIPU could elucidate that relationship. These clear differences in the effects of springflow between these two similar, co-occurring species emphasize the importance of springflow for CSRB. This relationship is illustrated across localities in Fig. 13 and indicates that maintaining springflow is essential to sustaining CSRB subpopulations. In Spring Run 1, following the one individual we found in May 2023, the ongoing drought and low-to-zero springflow in that locality has resulted in the absence of CSRB there through December 2024 (BIO-WEST unpublished data). Our modeled relationships between springflow and CSRB apparent occupancy and relative abundance are directly applicable to the range of environmental conditions observed during our study period; extrapolation of the model beyond the observed conditions may not accurately reflect the relationship of CSRB to springflow at higher or lower flows. Future research is needed to investigate flow-ecology relationships at springflow conditions near (or above) historic averages.

The time period in which we conducted this study was incredibly beneficial towards understanding CSRB responses to environmental conditions. We can reasonably assume that at total system springflows above those we experienced (>205 cfs), CSRB populations either continue to increase (at least to a saturation point) or remain stable. Therefore, the relationship between CSRB relative abundance and springflow that we have elucidated at lower springflows has helped to understand how this species is affected as the Comal Springs system dries. We recorded that as flows declined, reaching some of the lowest springflows observed during the past 30 years, CSRB relative abundance at Spring Island declined less dramatically than at Spring Run 3 and the Western Shoreline. The exception in on our model results is Spring Run 1 (Fig. 13), where the point at which a stable population declines towards zero may have been at local springflows above any that we experienced in our study or that have been observed since 2021. Better understanding of the relationship between springflow and CSRB relative abundance in Spring Run 1 (and Spring Run 2, which we did not examine), would require further study. Additionally, given the dominant effect of local springflow and relatively similar performance of models excluding biofilm, further inference regarding the relationship between CSRB and local springflow may be discerned by conducting a broader analysis using the long-term biomonitoring data.

5.3 Applicability to biomonitoring

The framework and its results described in sections 3.3d and 4.3c for applying our model results towards CSRB biomonitoring illustrates its utility for assessing whether observed CSRB relative abundance meets expectations based on our covariates. In our example, we utilized data from fall 2024 biomonitoring, which occurred during the period of lowest springflow during biomonitoring efforts since the program began (similar springflows to those observed during summer 2023 in this study). In one regard, the prevalence of zeros across 90% of sites and calculated relative abundance of 0 across localities should be expected given the low flows. However, it also illustrates the limitations of the model and our existing data of CSRB populations, as we do not have lure data from total system springflows below 55 cfs.

This framework can be used as part of a two-step process for assessing the results of semiannual biomonitoring. The first step, not presented in the methods for the framework, is a modification of the current way in which results are presented in the annual report, which is currently just a visual comparison of current-year averages to long-term averages. Here, the overall status of the population can be assessed by determining whether the relative abundance in each of the three monitored localities (Spring Island, Spring Run 3, Western Shoreline) fits within a given error (e.g., 1 standard deviation) that locality's historic relative abundance when total system springflows were within one standard deviation of their long-term average. This will determine whether current relative abundances match historic averages within each locality or not.

Second, our model and the framework illustrated here can be employed to determine whether the observed values of our covariates explain the observed relative abundances. If the observed relative abundance does not fall within the range of expected values, then some other factor could be having an effect on CSRB populations. Given that the main effect we observed (local springflow) is calculated based on measurements that are not required to be taken at the time of CSRB sampling, along with the similar performance of models without inclusion of the biofilm covariate (discussed in section 5.2), the framework for assessing the biomonitoring program is simpler than may be expected. It could potentially be justified to simplify data collection during biomonitoring to just beetle counts, collection timeframes, and locations, but further analysis of additional data would be needed before such a change is justified. While most covariates may not have had an effect in this study, it does not mean they may not in the future as more data across a wider range of conditions are collected.

The current biomonitoring program sets 30 lures (10 per locality) each spring and fall and has been consistent for 21 years. Under historically normal springflow conditions when relative abundance and occupancy are higher in all localities, it is possible that 30 lures would be more than effective at assessing the status of CSRB populations and could possibly be assessed with fewer lures in each locality. However, this is complicated when flows are lower as was illustrated by the fall 2024 biomonitoring results. Only 3 out of 30 sites had adult CSRB and 26 of the 31 beetles were on a single lure. With a reduced sampling program, you could easily have found no CSRB on all lures. While the model results in both situations would have produced a relative abundance of zero, a recorded abundance of zero would be alarming.

Similarly, maintaining two biomonitoring sampling events per year accounts for potential changes in CSRB populations with seasonal differences in total system springflow.

Further analysis of existing data could be explored to determine what number of lures could be set during biomonitoring while still maintaining the same accuracy as results obtained from ten lures per locality. For instance, if simulations suggest that sampling with five lures per locality twice per year achieves relative abundance values equal to ten lures per locality in 95% of simulations under normal flow conditions, then a change to the biomonitoring program could easily be justified. The five sites could be randomly selected during each sampling event from among the ten existing sites to eliminate biases from potentially selecting the most productive sites (such as the one Spring Island site that has consistently produced the most adult CSRB over the past two years). If flows are low during semiannual biomonitoring, setting lures at all 30 sites may be justified to adequately assess the status of the population. However, the current strategy for sampling during low flow conditions (3 lures in each of the 3 localities) may help maintain adequate detection capability when occurring before and/or after routine biomonitoring.

Maintaining a ~30-day sampling interval using cotton lures is prudent given the response of CSRB to biofilm that we document here. Shorter sampling intervals may be less likely to detect CSRB or adequately assess their abundance, while longer sampling intervals may result in degraded lures. This includes sampling during low-flow conditions, which during 2022 and part of 2023 were conducted every ~15 days. This both allows for biofilm development and limits unnecessary disturbance to each spring site. However, one justification for shorter sampling intervals could be if springflow rapidly dropped from an already low level during the sampling period (such as from 55 to 30 cfs).

The cotton lure methodology and preceding methods have now been used for over 20 years. Recent work (BIO-WEST 2025) suggests alternative “luring” methods using conditioned wood discs may be equally as effective at assessing CSRB abundance (including larvae; see section 5.2) and potentially more effective at assessing CSRB presence. However, further study and analysis of the two methods is needed to assess their comparability, as well as the long-term durability and other potential complicating factors of the wood discs before methods are changed. Maintaining consistent methodology for CSRB data collection should be prioritized until such comparisons are made to ensure methods are consistent and data are reliably comparable.

5.4 Conclusions and further recommendations

With the completion of this study and our review of its findings and the current state of CSRB knowledge, several recommendations can be made for potential future work to fill gaps in our understanding of this species. The key results of this study are 1) both adult and larval CSRB are readily found throughout the year and across nearly all active spring sites in Spring Run 3, Spring Island, and the Western Shoreline, but less is known about the species in Spring Runs 1 and 2; 2) local springflow had a dominant effect on CSRB relative abundance and occupancy across each of these three localities, while biofilm also had a positive effect; and 3) the current collection techniques and models developed here can be used to track and assess CSRB populations over time in the biomonitoring program.

The primary finding of our study was that springflow was the most important factor affecting CSRB relative abundance – CSRB populations in each locality of the Comal Springs system decline as local springflow declines. This relationship, which was not present in the similar co-occurring species, MIPU, emphasizes the importance of maintaining springflow and the associated stable environmental conditions, which showed little to no variation in our study. How this relationship between springflow and relative abundance translates to higher total system springflows and localized springflows in Spring Runs 1 and 2 should be explored further. In the three primary localities, this should be examined by using existing long-term monitoring data and calculating local springflow averages for the entirety of the timeseries. This can be supplemented through a limited study (e.g., one or two sampling events) during time periods when total system springflows remain consistently near or above 300 cfs using all (or most) of the sites included in this study. Data from such a limited repeat study could be combined with data from this study for a more comprehensive assessment CSRB relative abundance over a full range of springflows. A supplemental study like this, or others, could occur at any time of year since we see no indication of phenological variation in abundances of each life stage.

Subpopulations of CSRB in Springs Runs 1 and 2 should be given further consideration, especially in the light of the current drought and potential loss of the population in Spring Run 1. A limited incorporation of each of these localities into the semiannual biomonitoring program (e.g., 3 lures per locality) would go a long way to improving our understanding of the species in those localities. Lure data from these localities have been very limited and sporadic over the past 20 years. More detailed monitoring of Spring Run 1 if/when local springflows consistently return to higher levels could provide valuable data on recolonization following drought. While Spring Run 1 might not support a genetically unique population or be critical to the overall species survival, understanding the response of CSRB there following drought would be valuable to know if a more severe drought were to similarly impact Spring Runs 2 and 3. Similarly, initial data have suggested that CSRB remain near the substrate – water interface (BIO-WEST unpublished data), but further study could confirm this hypothesis.

Although we did not identify other environmental characteristics that have clear effects on CSRB populations, the positive effect of lure biofilm suggests there could be some other characteristic of individual spring sites that indirectly affected our results by affecting the amount of biofilm on lures. This could be something such as local microbial communities that are shaped by plant species with roots near the spring or inputs of certain other types of organic material at each spring location. Detailed microbial assessment of objects occurring in springs and lures would be necessary for making this connection. Other than local springflow, the lack of clear environmental factors affecting CSRB populations is perhaps a greater reflection on the fact that CSRB is a spring-endemic species and adapted to stable environmental conditions that otherwise show little to no variation across its range. This same pattern may be expected of other spring-associated invertebrates, but every species is different and even closely related species can have contrasting responses to environmental conditions as they have evolved to fill their own niche. While the results of this study can be used to inform future studies of other species, the biology of each species should carefully be considered when designing other studies.

The results, models, and framework developed in this study should be used to formalize an annual assessment of CSRB using biomonitoring data. This will enable tracking of the status of CSRB populations and if their relative abundance matches predictions based on springflow. Additional analysis of existing data can be used to assess the efficiency of the sampling program and potentially refine the strategy behind the number of lures and their distribution throughout the system during biomonitoring to maximize resource use and meaningful data collection. This analysis of the biomonitoring program, combined with the additional studies suggested above, are warranted to accomplish the overall goals of the EAHCP – to track and protect these endemic invertebrates over time.

6. Acknowledgements

This project was funded by the Edwards Aquifer Authority contract #21-019-TES. We thank the EAHCP Science Committee CSRB working group for the discussions that helped design the study, Andy Royle (USGS) for providing guidance and reviewing our design and statistical methods, Katie Bockrath and Braden West (USFWS San Marcos Aquatic Resources Center) for assisting with beetle processing in the field, and Israel Prewitt and Logan Leedham (BIO-WEST) for assistance with conducting field work. All work with endangered species was conducted under BIO-WEST permits #ES037155 from the U.S. Fish and Wildlife Service and #SPR-0101-131 from the Texas Parks and Wildlife Department.

7. References

Bartoń, K. 2020. MuMIn: Multi-model inference.

BIO-WEST. 2025. Comal Springs dryopid beetle (*Stygoparnus comalensis*) research 2023–2024: laboratory studies of habitat preferences and development of field methods for detection, collection, and monitoring. San Marcos, TX.

Bosse, L. S., D. W. Tuff, and H. P. Brown. 1988. A new species of *Heterelmis* from Texas (Coleoptera: Elmidae). The Southwestern Naturalist 33:199–203.

Bowles, D. E., and T. L. Arsuffi. 1993. Karst aquatic ecosystems of the Edwards Plateau region of central Texas, USA: a consideration of their importance, threats to their existence, and efforts for their conservation. Aquatic Conservation: Marine and Freshwater Ecosystems 3:317–329.

Bowles, D. E., C. B. Barr, and R. Stanford. 2003. Habitat and phenology of the endangered riffle beetle *Heterelmis comalensis* and a coexisting species, *Microcylloepus pusillus*, (Coleoptera: Elmidae) at Comal Springs, Texas, USA. Archiv für Hydrobiologie 156:361–383.

Brooks, M. E., K. Kristensen, K. J. van Benthem, A. Magnusson, C. W. Berg, A. Nielsen, H. J. Skaug, M. Maechler, and B. M. Bolker. 2017. glmmTMB balances speed and flexibility among packages for zero-inflated generalized linear mixed modeling. The R Journal 9:378–400.

Brune, G. 2002. Springs of Texas: Volume 1. Second edition. Texas A&M University Press, College Station.

Cooke, M., G. Longley, and R. Gibson. 2015. Spring association and microhabitat preferences of the Comal Springs riffle beetle (*Heterelmis comalensis*). The Southwestern Naturalist 60:110–121.

De Cicco, L. A., R. M. Hirsch, D. Lorenz, W. D. Watkins, and M. Johnson. 2024. dataRetrieval: R packages for discovering and retrieving water data available from Federal hydrologic web services.

(EAHCP) Edwards Aquifer Habitat Conservation Plan. 2012. Edwards Aquifer Recovery Implementation Program: Habitat Conservation Plan. Page 414. Edwards Aquifer Authority, San Antonio, TX.

Edwards Aquifer Authority. 2016. Comal Springs Riffle Beetle Cotton Lure SOP. Edwards Aquifer Authority.

Fries, J. N. 2003. Possible reproduction of the Comal Springs riffle beetle, *Heterelmis comalensis* (Coleoptera: Elmidae), in captivity. Entomological News 114:7–9.

Gelman, A., J. B. Carlin, H. S. Stern, D. B. Dunson, A. Vehtari, and D. B. Rubin. 2013. Bayesian Data Analysis. Third edition. Chapman and Hall, Boca Raton.

Gelman, A., and D. B. Rubin. 1992. Inference from iterative simulation using multiple sequences. Statistical Science 7:457–511.

Gibson, J. R., S. J. Harden, and J. N. Fries. 2008. Survey and distribution of invertebrates from selected springs of the Edwards Aquifer in Comal and Hays Counties, Texas. The Southwestern Naturalist 53:74–84.

Hobbs, N. T., and M. B. Hooten. 2015. Bayesian Models: A Statistical Primer for Ecologists. Princeton University Press, Princeton, NJ.

Huston, D. C., and J. R. Gibson. 2015. Underwater pupation by the Comal Springs riffle beetle, *Heterelmis comalensis* Bosse, Tuff, and Brown, 1988 (Coleoptera: Elmidae), with an update on culture techniques. The Coleopterists Bulletin 69:521–524.

Huston, D. C., J. R. Gibson, K. G. Ostrand, C. W. Norris, and P. H. Diaz. 2015. Monitoring and marking techniques for the endangered Comal Springs riffle beetle, *Heterelmis comalensis* Bosse, Tuff, and Brown, 1988 (Coleoptera: Elmidae). The Coleopterists Bulletin 69:793–798.

Hutchins, B. T. 2018. The conservation status of Texas groundwater invertebrates. Biodiversity and Conservation 27:475–501.

Kellner, K. 2024. jagsUI: A Wrapper Around “rjags” to Streamline “JAGS” Analyses.

Kéry, M., B. Gardner, and C. Monnerat. 2010. Predicting species distributions from checklist data using site-occupancy models. Journal of Biogeography 37:1851–1862.

Kosnicki, E. 2022. Fecundity of first-generation captively reared *Heterelmis comalensis* (Coleoptera: Elmidae). Journal of Insect Science 22:1–3.

Lucas, L. K., Z. Gompert, J. R. Gibson, K. L. Bell, C. A. Buerkle, and C. C. Nice. 2016. Pervasive gene flow across critical habitat for four narrowly endemic, sympatric taxa. Freshwater Biology 61:933–946.

Lüdecke, D. 2018. ggeffects - Estimated Marginal Means and Adjusted Predictions from Regression Models. Journal of Open Source Software 3:772.

Mays, Z., A. Hunter, L. G. Campbell, and C. Carlos-Shanley. 2021. The effects of captivity on the microbiome of the endangered Comal Springs riffle beetle (*Heterelmis comalensis*). FEMS Microbiology Letters 368:fnab121.

Nair, P., P. H. Diaz, and W. H. Nowlin. 2021. Interactions at surface–subterranean ecotones: structure and function of food webs within spring orifices. Oecologia 196:235–248.

Nair, P., J. R. Gibson, B. F. Schwartz, and W. H. Nowlin. 2023. Temperature responses vary between riffle beetles from contrasting aquatic environments. Journal of Thermal Biology 112:103485.

Nakagawa, S., and H. Schielzeth. 2013. A general and simple method for obtaining R^2 from generalized linear mixed-effects models. Methods in Ecology and Evolution 4:133–142.

National Academies of Sciences, Engineering, and Medicine. 2018. Review of the Edwards Aquifer Habitat Conservation Plan: Report 3. Page 25200. National Academies Press, Washington, D.C.

Polášková, V., J. Bojková, M. Polášek, V. Šorfová, and M. Horsák. 2022. Water temperature stability modulates insect thermal responses at spring fens. Hydrobiologia 849:4693–4706.

R Core Team. 2024. R: A Language and Environment for Statistical Computing. R Foundation for Statistical Computing, Vienna.

Royle, J. A. 2004. *N* -mixture models for estimating population size from spatially replicated counts. Biometrics 60:108–115.

Royle, J. A., and R. M. Dorazio. 2008. Hierarchical Modeling and Inference in Ecology: The Analysis of Data from Populations, Metapopulations and Communities. Academic Press, Burlington, MA.

Tyers, M. 2024. jagshelper: Extracting and Visualizing Output from “jagsUI.”

United States Fish and Wildlife Service. 1997. Endangered and threatened wildlife and plants; final rule to list three aquatic invertebrates in Comal and Hays counties, TX, as endangered. Federal Register 62:66295–66304.

United States Fish and Wildlife Service. 2013. Endangered and threatened wildlife and plants; revised critical habitat for the Comal Springs dryopid beetle, Comal Springs riffle beetle, and Peck’s cave amphipod. Federal Register 78:63100–63127.

United States Fish and Wildlife Service. 2022. Captive Husbandry and Propagation of the Comal Springs Riffle Beetle: 2022 Research Report for the Edwards Aquifer Authority. Page 25. San Marcos, TX.

United States Fish and Wildlife Service. 2024. Comal Springs Riffle Beetle (*Heterelmis comalensis*) 5-Year Status Review: Summary and Evaluation. Page 47. Austin Ecological Services Field Office, Austin, TX.

Wickham, H., W. Chang, L. Henry, T. L. Pedersen, K. Takahashi, C. Wilke, K. Woo, H. Yutani, D. Dunnington, and T. van den Brand. 2024. ggplot2: Elegant Graphics for Data Analysis. Springer.

Zera, A. J., and R. F. Denno. 1997. Physiology and ecology of dispersal polymorphism in insects. Annual Review of Entomology 42:207–230.

8. Appendix

Figure S1. Photograph of the seepage meter in use at an upwelling site in the Spring Island area.

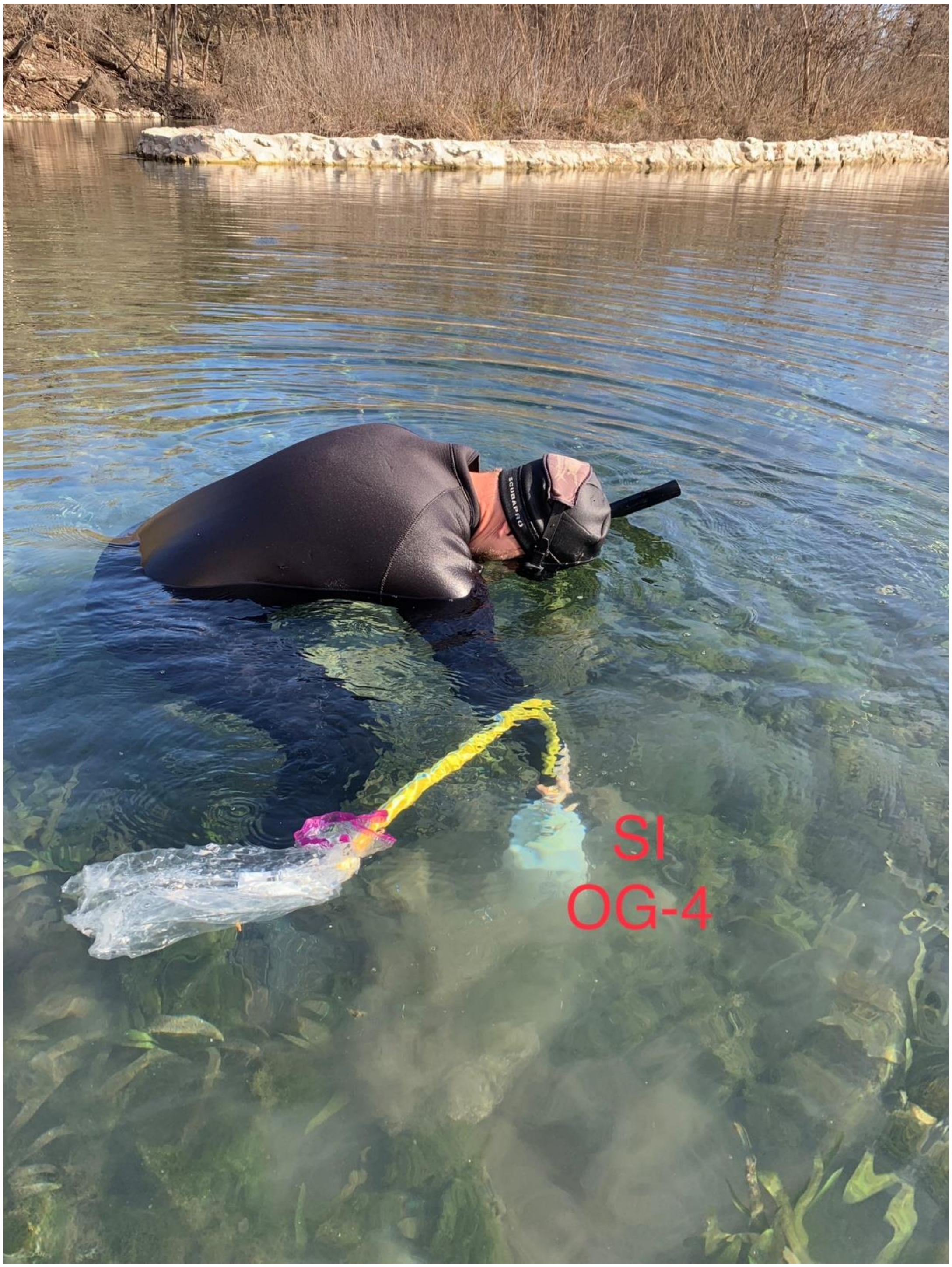

Figure S2. Scatterplot of 51 measurements for which there were measurements of both flow (cm/s) measured with the Hach flow meter and flux (mL/cm^2/s) measured with the seepage meter at upwelling sites. This relationship was used to convert flux measurements into approximate flow measurements for direct comparison of the two methods.

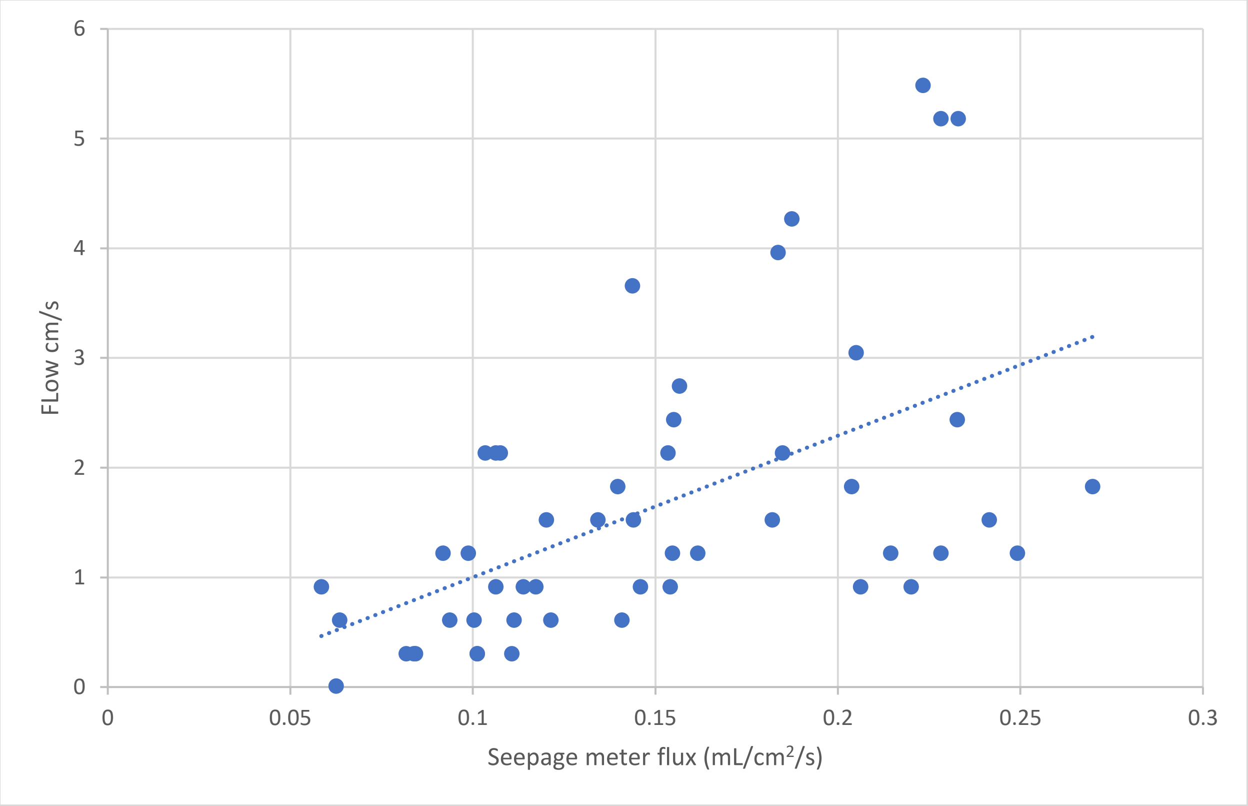

Figure S3. Map of sectors (spatial groupings of sites) at Spring Island.

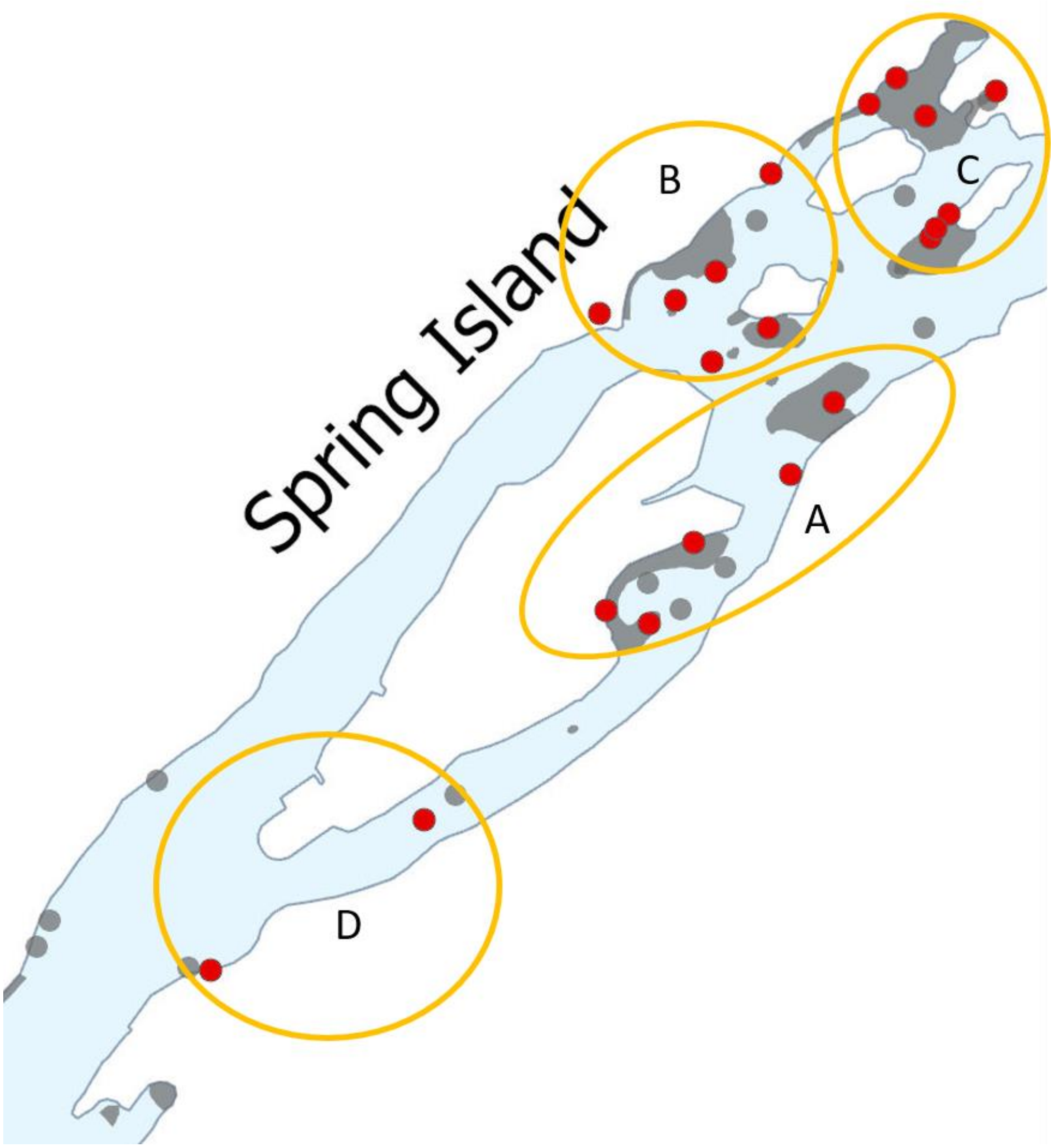

Figure S4. Map of sectors (spatial groupings of sites) at Spring Runs 1 and 3.

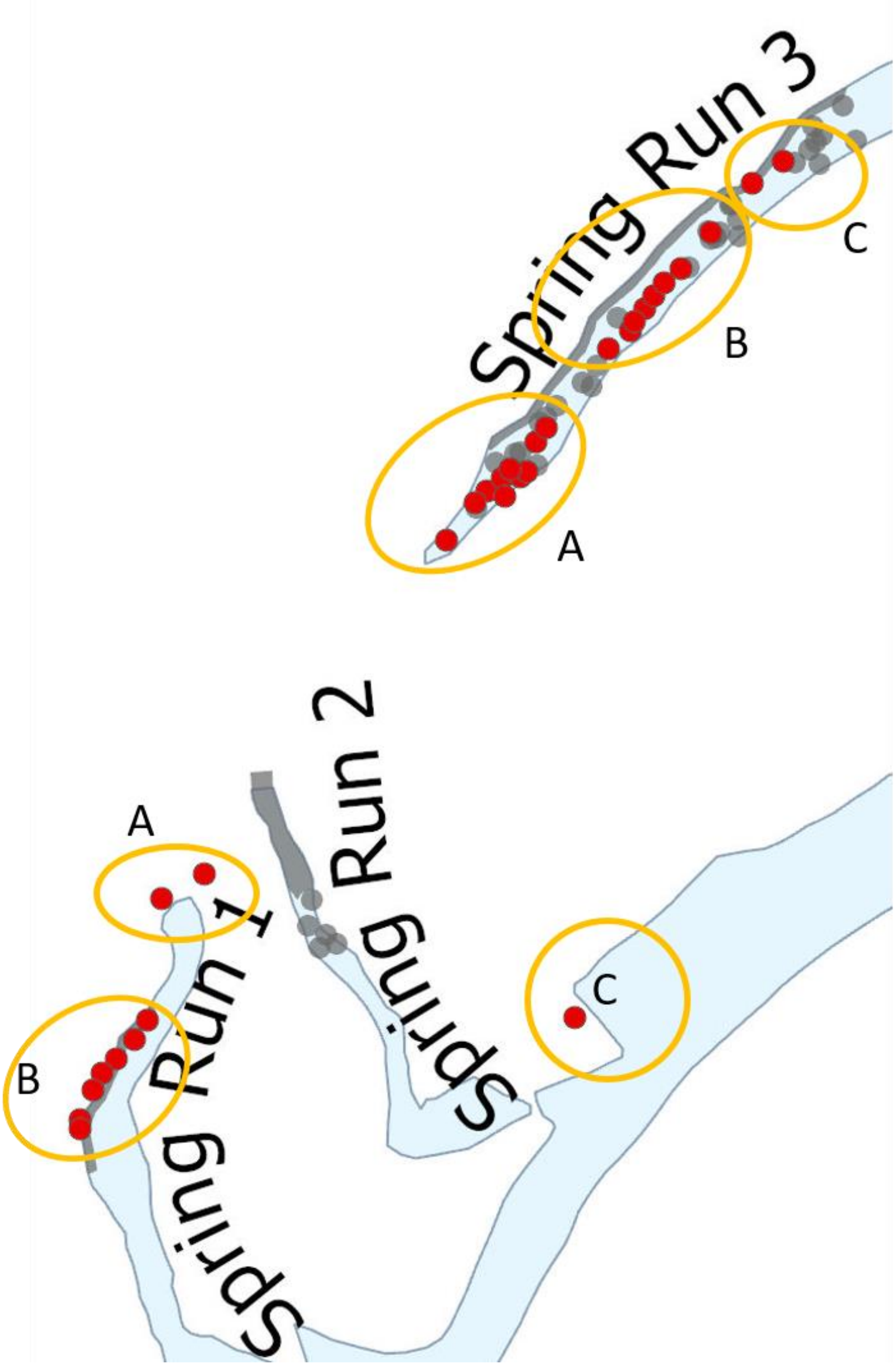

Figure S5. Map of sectors (spatial groupings of sites) at the Western Shoreline.

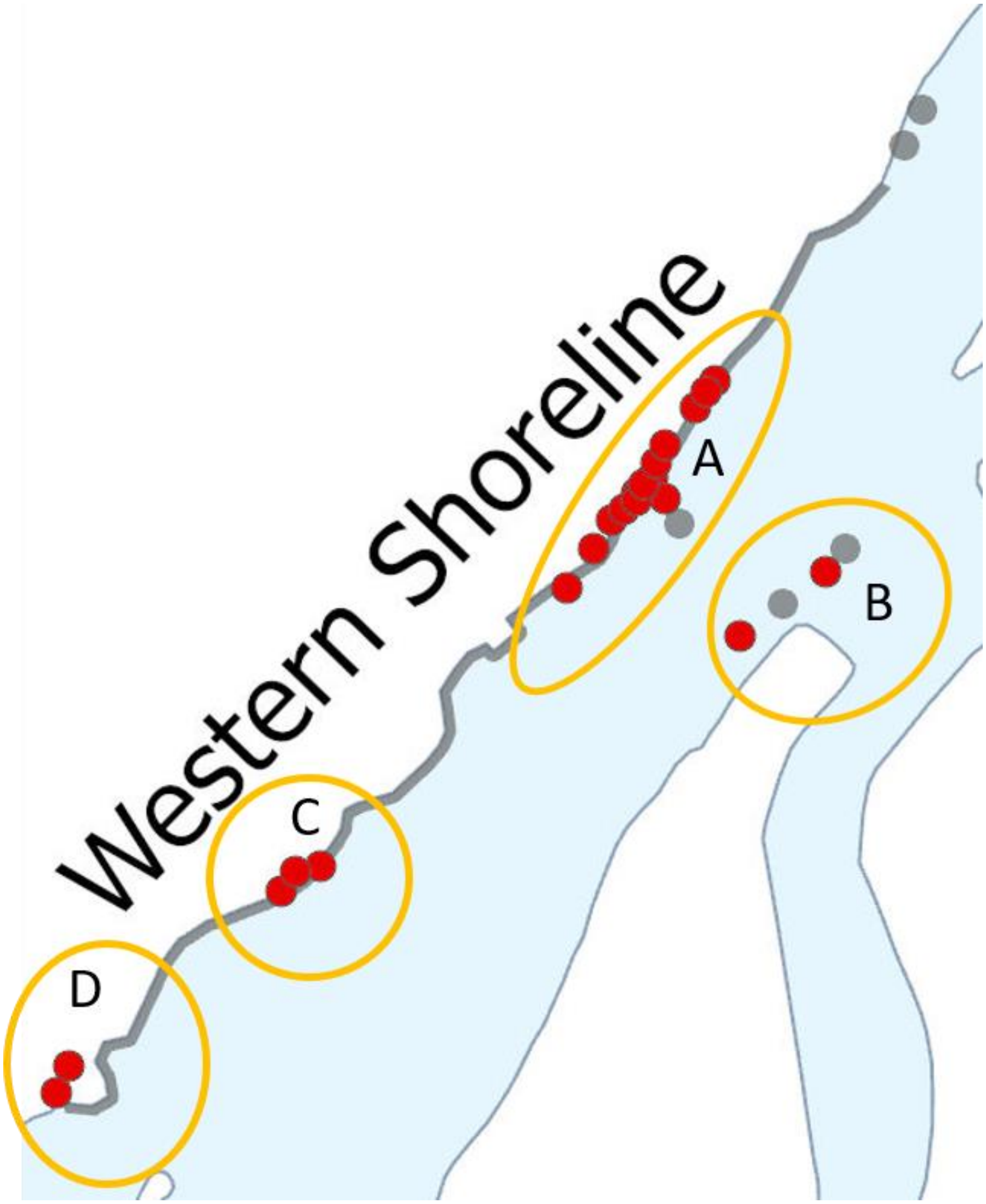

Figure S6. Mean (±SE) of the natural log transformed number of CSRB adults in the three primary sampling localities (excluding Spring Run 1) over the course of the study (by sampling period).

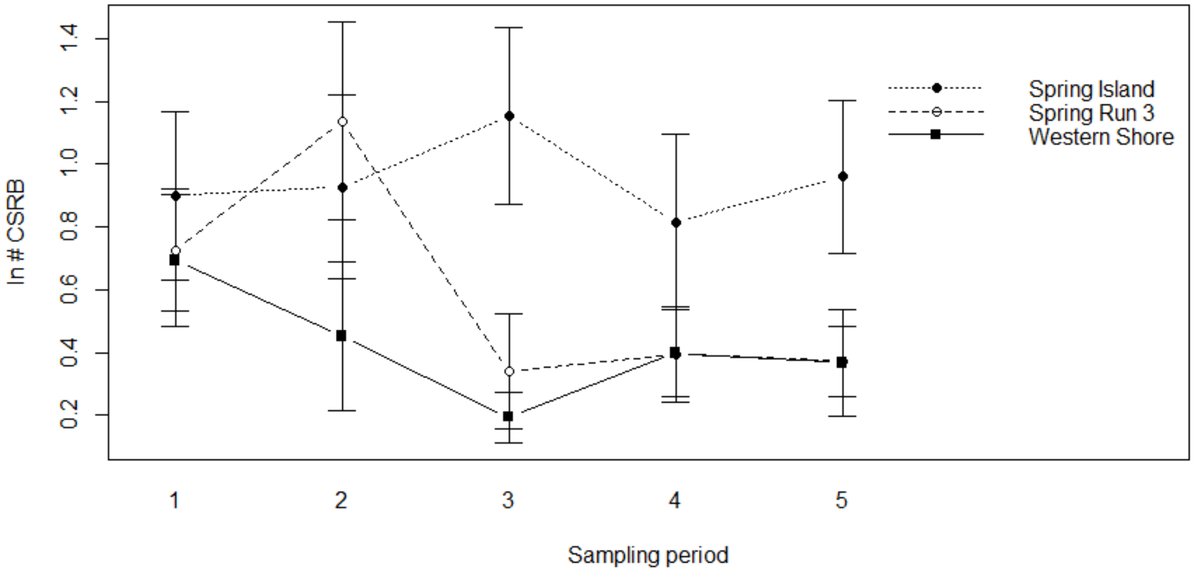

Figure S7. Mean (±SE) of the natural log transformed number of CSRB larvae in the three primary sampling localities over the course of the study (by sampling period).

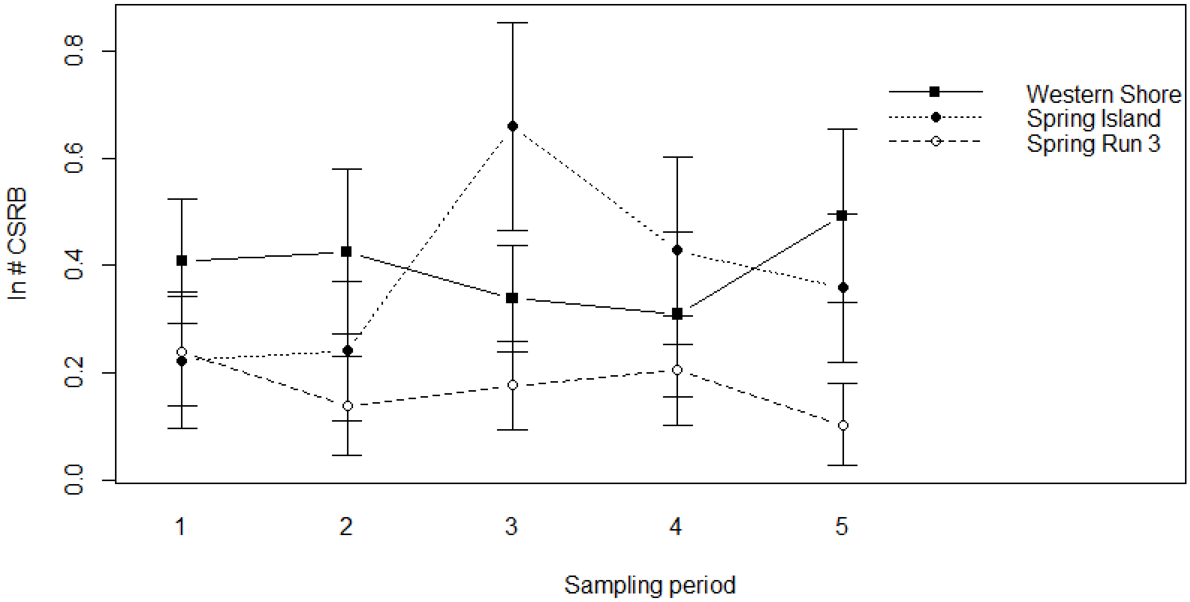

Figure S8. Mean (±SE) of the natural log transformed number of MIPU adults in the three primary sampling localities over the course of the study (by sampling period).

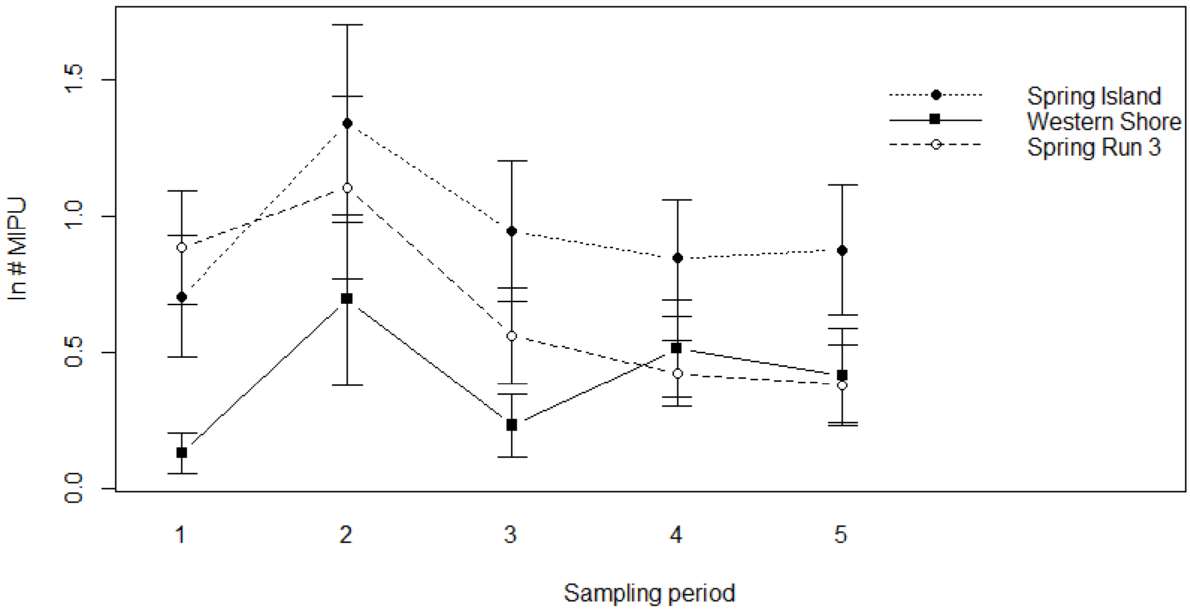

Figure S9. Mean (±SE) of the natural log transformed number of MIPU larvae in the three primary sampling localities over the course of the study (by sampling period).

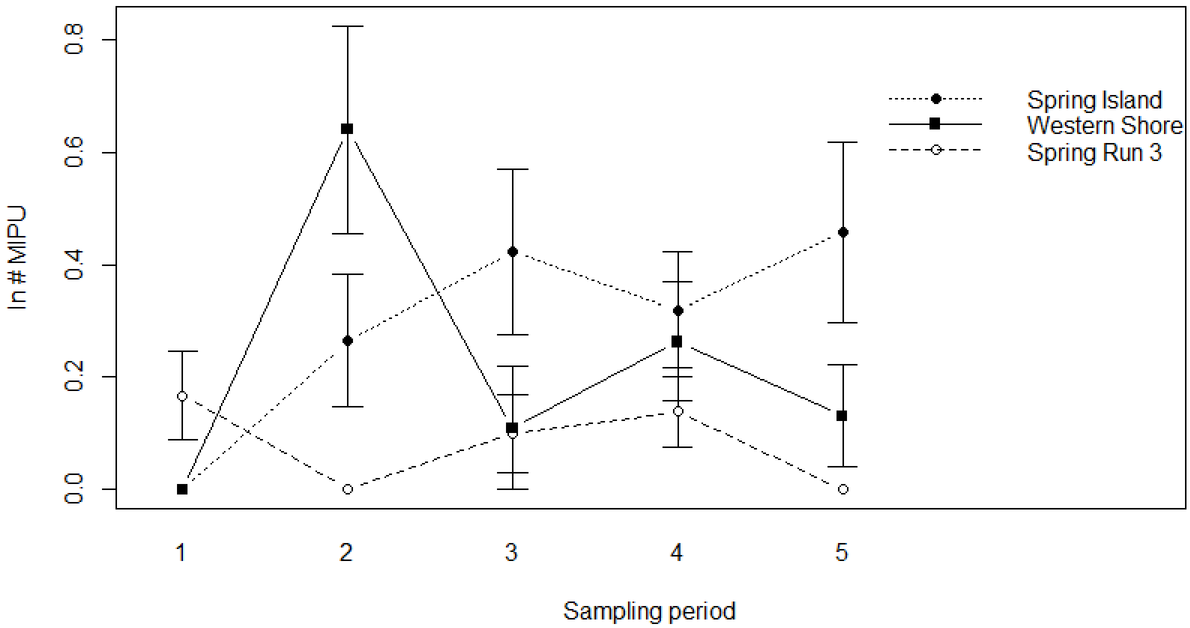

Figure S10. Boxplots of dissolved oxygen by locality and sampling period when lures were set.

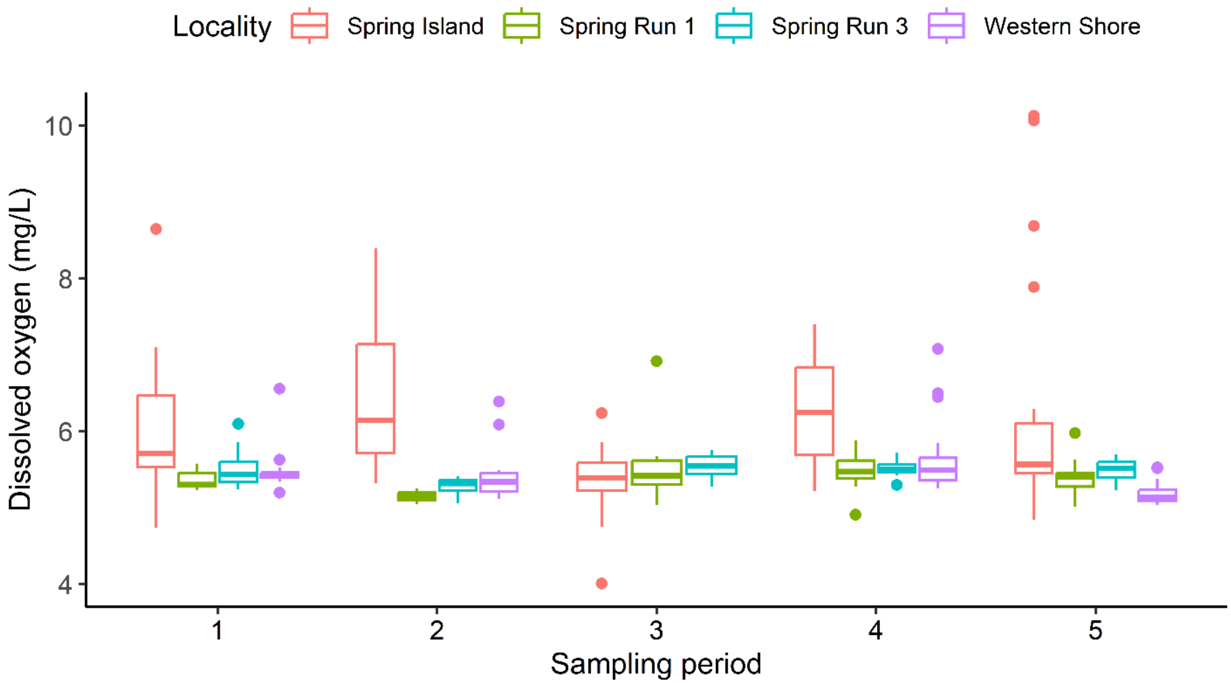

Figure S11. Boxplots of conductivity by locality and sampling period when lures were set.

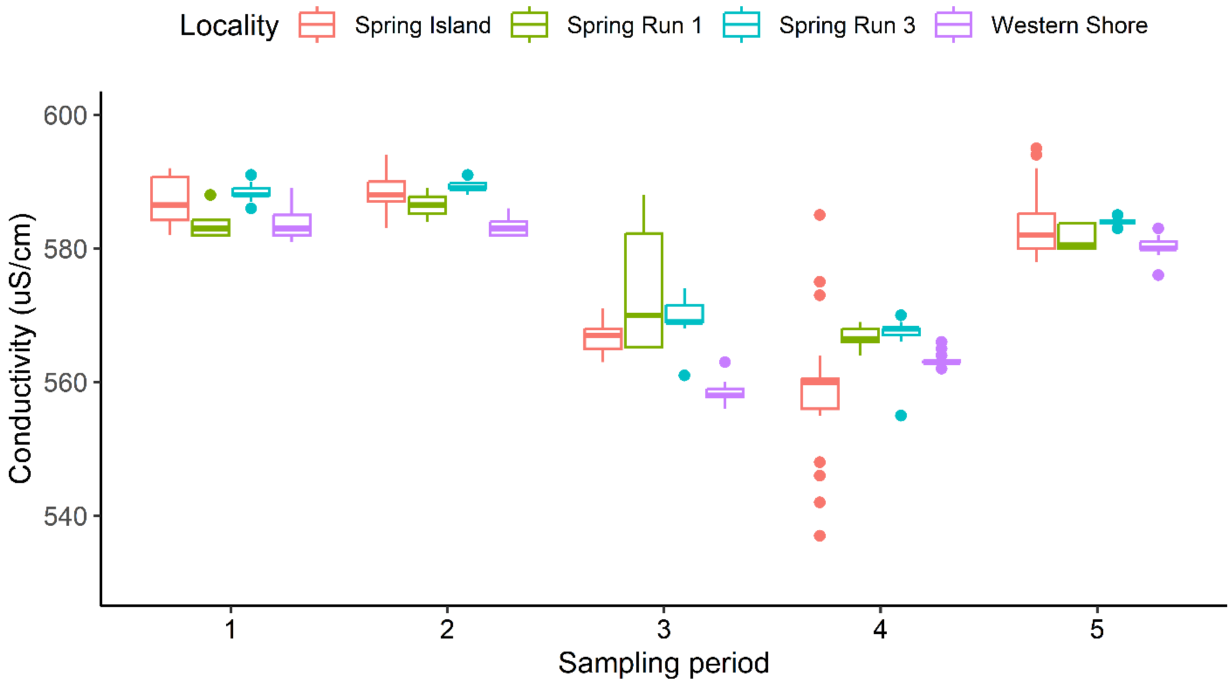

Figure S12. Boxplots of temperature by locality and sampling period when lures were set.

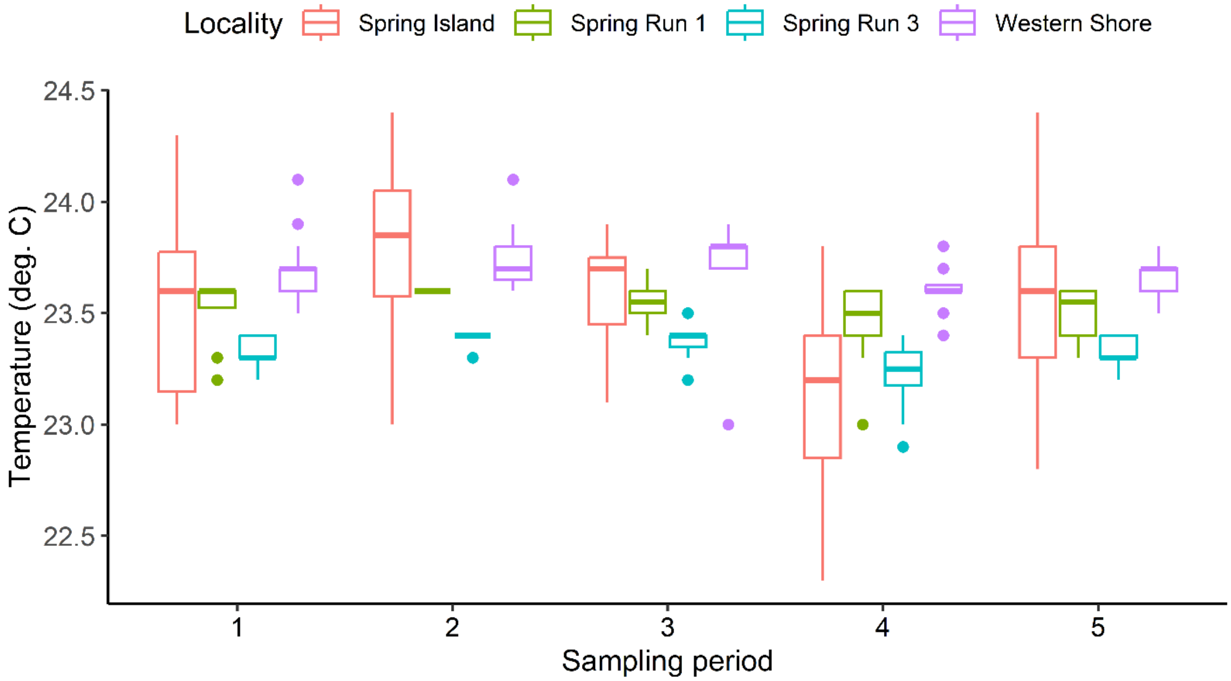

Figure S13. Boxplots of lure depth by locality when lures were set.

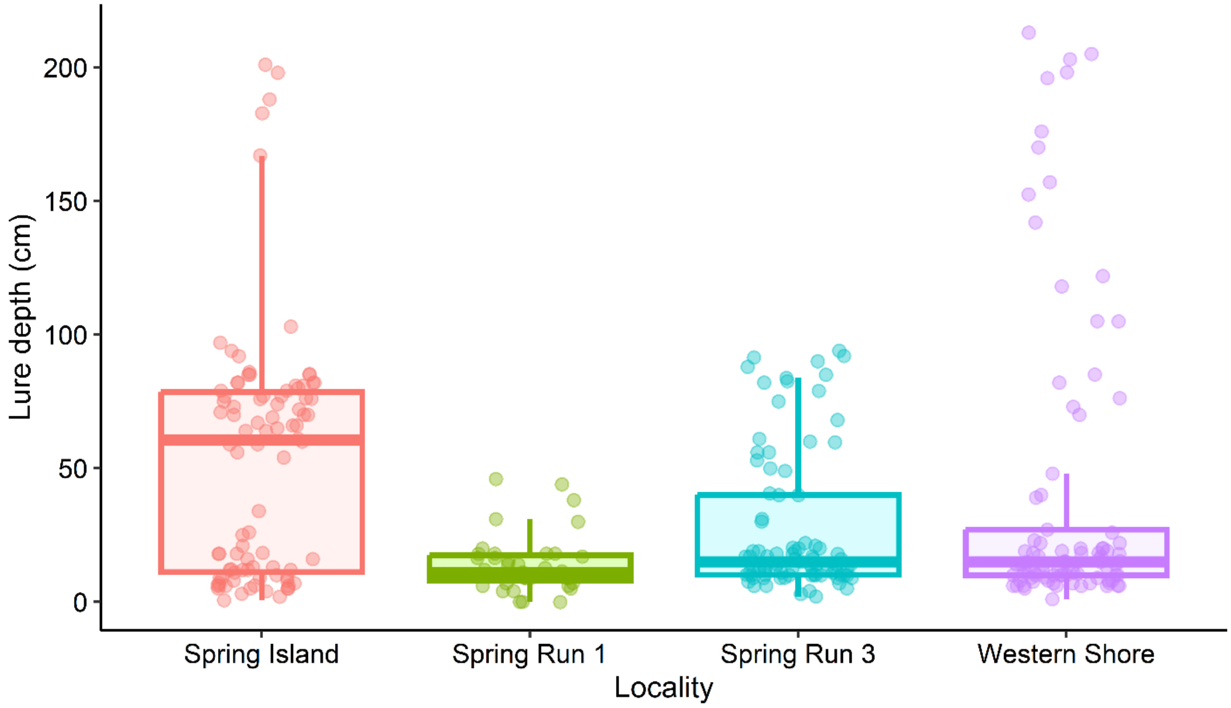

Figure S14. Boxplots of average substrate size by locality when lures were set. Points near the same y value generally are from the same site across different sampling periods.

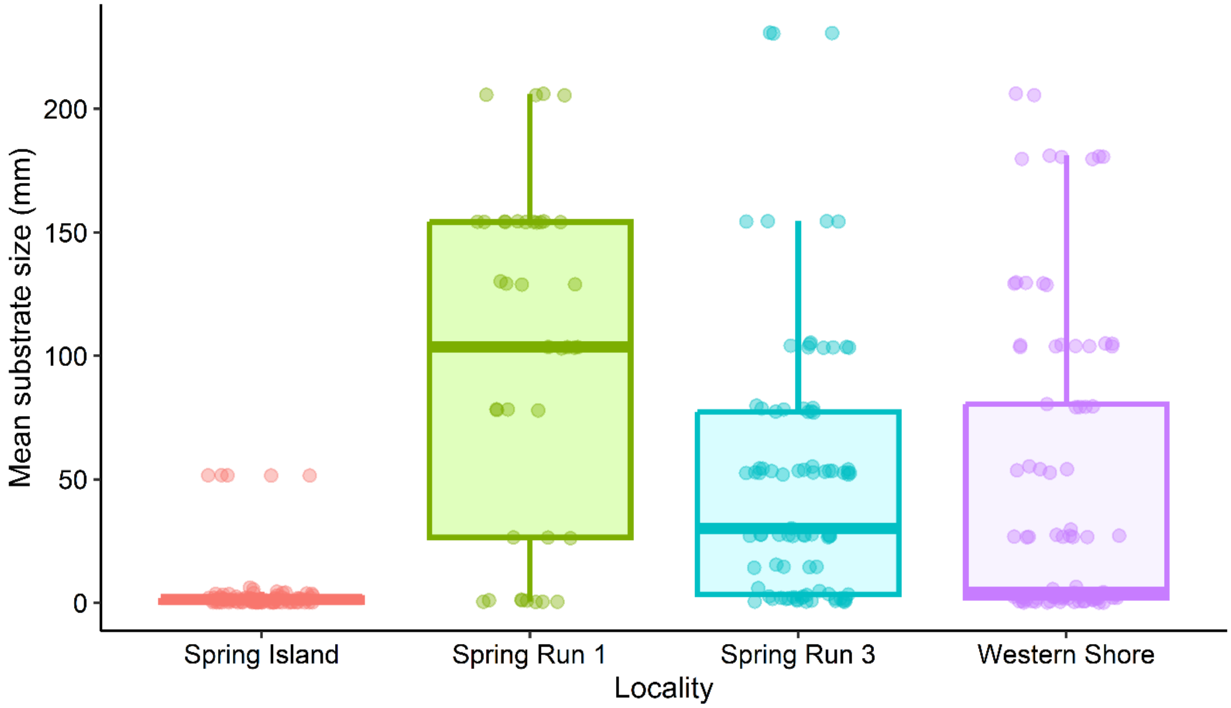

Figure S15. Scatterplot of the natural log-transformed number of CSRB adults versus average site-level springflow.

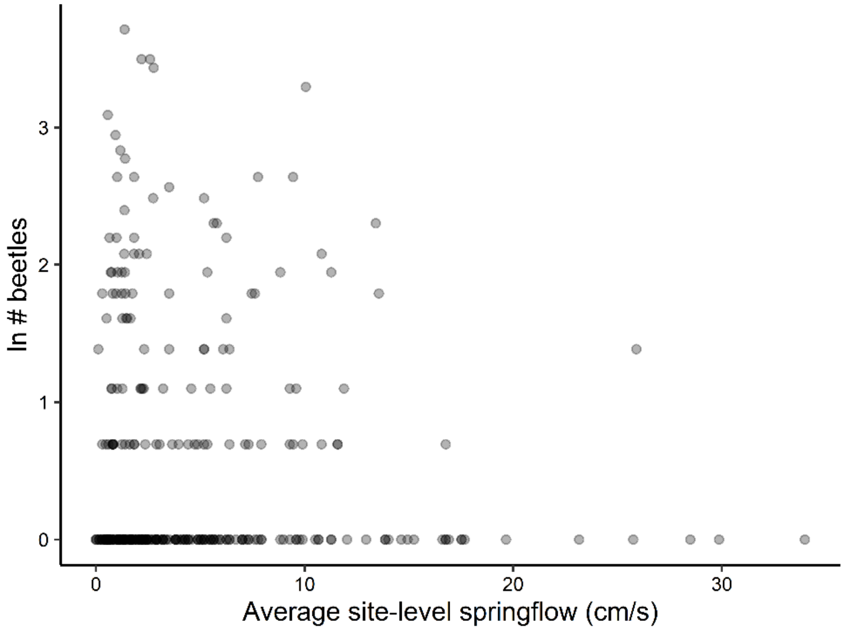

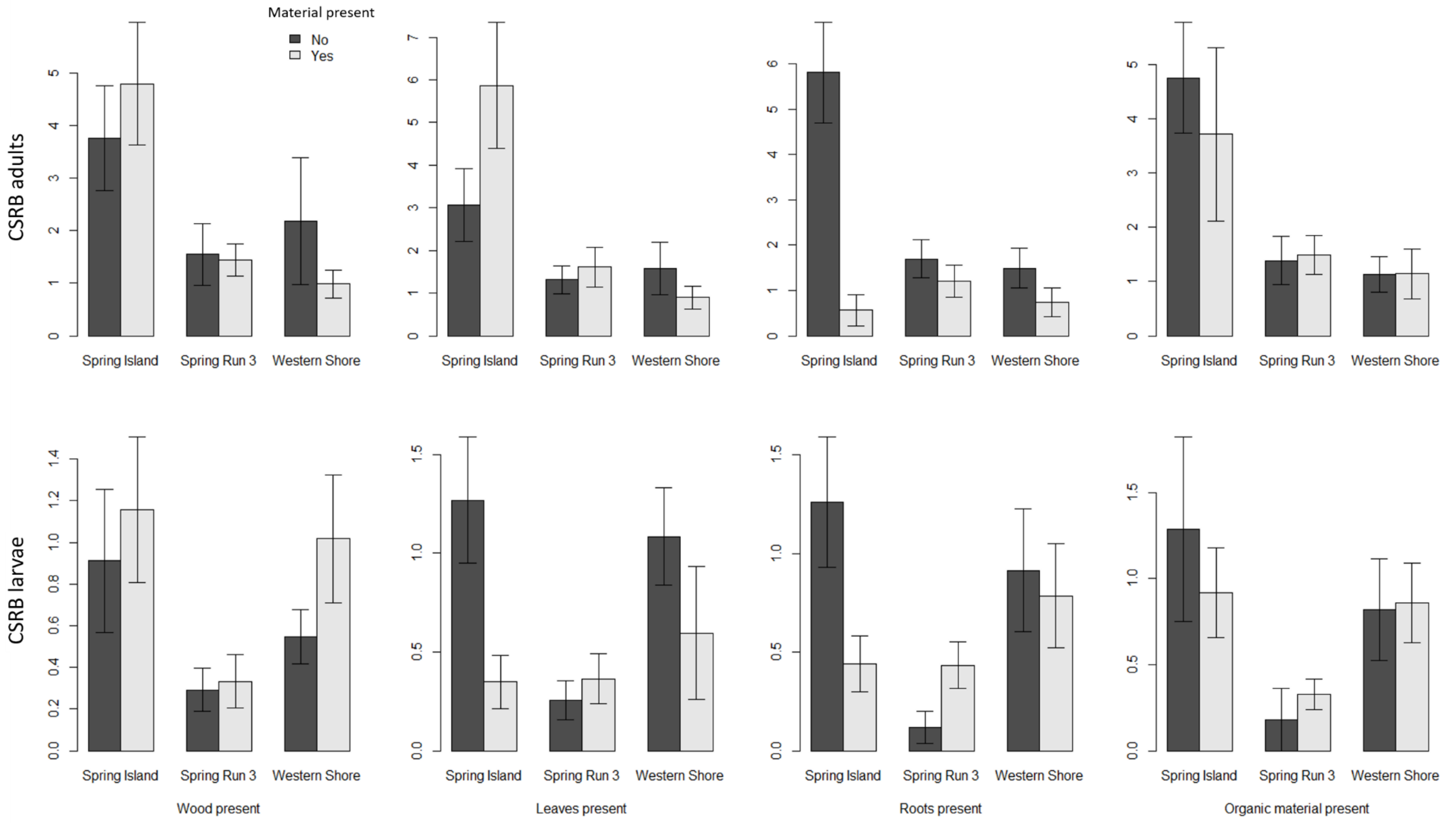

Figure S16. Mean (±SE) CSRB adult and larval abundance by locality (excluding Spring Run 1) based on the presence/absence of wood, leaves, roots, or the three combined (all organic material).

Figure S17. Boxplots of total biofilm coverage on lures by locality and sampling period when lures were retrieved.

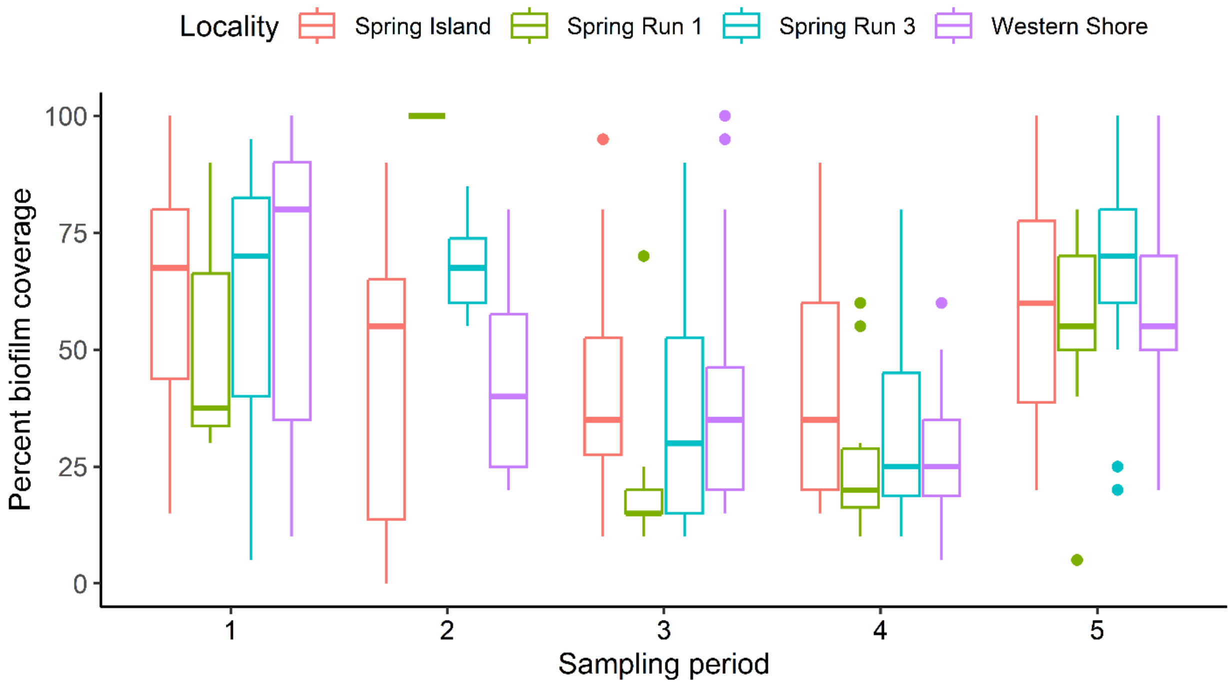

Table S1. Summary of deviance information criteria (DIC) and Bayesian p-values (B_p) for generalized linear mixed effects models with alternate parameterizations. Candidates include models with the intercepts only (Null-model), 30-day local springflow average covariate (SF), total biofilm covariate (TB), and both covariates included (SF + TB). Models with the lowest DIC scores were considered the best supported and highlighted in bold lettering.

	CSRB Adults		**CSRB Larvae**		**MIPU Adults**		**MIPU Larvae**	
	DIC	**B_p**	**DIC**	**B_p**	**DIC**	**B_p**	**DIC**	**B_p**
Null-model	719.99	0.48	521.36	0.50	707.60	0.50	319.75	0.51
SF	**716.57**	**0.49**	521.50	0.52	707.52	0.50	**307.91**	**0.51**
TB	735.92	0.45	**515.89**	**0.50**	702.23	0.50	316.28	0.50
SF + TB	741.42	0.45	519.24	0.52	**699.46**	**0.50**	311.99	0.51